STUDY OF RATCHETING BEHAVIOR OF METALLIC MATERIALS USING MOLECULAR DYNAMICS SIMULATION

Thesis submitted in the partial fulfillment of the requirement for the degree of

BACHELOR OF TECHNOLOGY

in

METALLURGICAL AND MATERIALS ENGINEERING

BY

NISHANT PRAKASH
(Roll No. 108MM024)
&
DHIRENDRA GAMANGO
(Roll No. 108MM049)

NATIONAL INSTITUTE OF TECHNOLOGY, ROURKELA
May, 2012

STUDY OF RATCHETING BEHAVIOR OF METALLIC MATERIALS USING MOLECULAR DYNAMICS SIMULATION

Thesis submitted in the partial fulfillment of the requirement for the degree of

BACHELOR OF TECHNOLOGY

in

METALLURGICAL AND MATERIALS ENGINEERING

BY

NISHANT PRAKASH
(Roll No. 108MM024)
&
DHIRENDRA GAMANGO
(Roll No. 108MM049)

Under the guidance of

PROF. KRISHNA DUTTA

NATIONAL INSTITUTE OF TECHNOLOGY, ROURKELA
May, 2012

NATIONAL INSTITUTE OF TECHNOLOGY ROURKELA

CERTIFICATE

This is to certify that the thesis entitled **"STUDY OF RATCHETING BEHAVIOR OF PURE COPPER AND PURE ALUMINUM USING MOLECULAR DYNAMICS SIMULATION"** submitted by **Nishant Prakash** (108MM024) and **Dhirendra Gamango** (108MM049) in partial fulfilment of the requirements for the award of **BACHELOR OF TECHNOLOGY** Degree in **Metallurgical and Materials Engineering** at the **National Institute of Technology, Rourkela** is an original work carried out by them under my supervision and guidance.

The matter embodied in the thesis has not been submitted to any other University/ Institute for the award of any degree.

Date: 10th May, 2012

Prof. Krishna Dutta
Assistant Professor
Dept. of Metallurgical and Materials Engineering,
National Institute of Technology Rourkela –
769008

ACKNOWLEDGEMENT

We avail this opportunity to epitomise our indebtedness to our guide Prof. Krishna Dutta, Department of Metallurgical and Materials Engineering, NIT Rourkela, for his valuable guidance, constant encouragement and kind help at all stages for the execution of this dissertation work.

We are also grateful to Prof. Natraj Yedla, Department of Metallurgical and Materials Engineering, NIT Rourkela for providing valuable assistance and insight during the simualation process.

We express our sincere gratitude to Prof. Dr. B. C. Ray, Head of the Department, Metallurgical and Materials Engineering, NIT Rourkela for giving us an opportunity to work on this project and allowing us access to valuable facilities in the department.

We would also like to thank Sanup Kumar Panda for their help and support through the course of our project work.

Date: 10th May, 2012

Nishant Prakash (108MM024)

Dhirendra Gamango (108MM049)

Dept. of Metallurgical and Materials Engineering,

National Institute of Technology, Rourkela

Rourkela-769008

CONTENTS

Chapter 1

INTRODUCTION

1. Introduction

***Alexander L. Kielland oil platform capsize*-The Alexander L. Kielland was a Norwegian semi-submersible drilling rig that capsized while working in the windyEkofisk oil field in March 1980 leading to 123 fatalities. This capsize was the worst disaster in Norwegian waters since World War II. In March 1981, the investigation team[1]concluded that the rig broke down owing to a fatigue crack in one of its six bracings, which connected the collapsed D-leg to the rest of the rig. Similarly, Versailles train crash and several other incidents, mostly airplane crashes have occurred due to failure by fatigue and by ratcheting deformation.**

Fatigue has always been a matter of great concern for material science researchers and engineers. It is the structural damage that occurs to a material under cyclic loading even when the applied stress is much below its ultimate tensile strength. Fatigue failure may be of different types, viz. low cycle fatigue, high cycle fatigue, very low cycle and very high cycle fatigue etc. [2]. Materials used in nuclear reactor chambers pose great risk from low cycle fatigue and specifically, ratcheting. Therefore, special care must be taken as consequences of fatigue failure of this type of materials could be dreadful. Therefore, extensive research works are being performed now-a-days.

Ratcheting is the phenomenon of accumulation of strain during asymmetric cyclic loading of materials under application of non-zero mean stress at different values of alternate stress [3–15]. This phenomenon is considerably important for the purpose of design and safety assessment of engineering components, as accumulation of ratcheting strain degrades fatigue life [8,9] of structural components. This may in turn limit the predictive capability of the well-known Coffin–Manson relation [7]. It is thus essential to understand ratcheting behavior of materials in order to protect engineering components or structures which may possibly get subjected to asymmetric cyclic loading. Over the past two decades, studies on the ratcheting behavior of materials have received significant attention by several investigators for both experimental data generation and simulation studies [17–26]. Several researches have been done on the effects of mean stress (σm), stress amplitude (σa), temperature (T) and material chemistry on the

ratcheting strain ($\varepsilon\rho$) and ratcheting strain rate ($\dot{\varepsilon}_r$). Most of the existing investigations are based on experimental results and findings. Reports are also available based on simulation of ratcheting behavior through mathematical models. To do an experiment related to ratcheting is quite time-consuming and a well-equipped laboratory set-up is required.

Computer based molecular dynamics (MD) simulation is now-a-days potentially utilized to study different material behaviors. Computer simulations act as a channel between microscopic length and time scales and the macroscopic world of the laboratory. It provides a guess at the interactions between molecules, and exactly predicts the bulk properties. The predictions can be made as precise and accurate as we like, subject to the limitations imposed by our computer's ability. At the same time, the concealed detail behind bulk measurements can be revealed. Although, MD simulation is being used to predict low cycle fatigue behavior of Ti-alloys, it has not been used to predict ratcheting behavior of materials, as per the best knowledge of the authors.

We carry out computer simulations in order to understand the properties of cluster of molecules in terms of their structure and the microscopic interactions. This serves as a counterpart to conventional experiments, enabling us to find out something new, that cannot be discovered in other ways. Molecular dynamics is a computer simulation of physical movements and interactions of atoms and molecules. For a period of time the atoms and molecules are allowed to interact, giving a view of the atomic movements. In the most common version, the molecules and atoms are traced by numerically solving the Newton's equations of motion for a system of interacting particles, where forces between the particles and potential energy are outlined by molecular mechanics force fields. The method was originally devised within theoretical physics in the late 1950s and early 1960s, but is applied today mostly in materials science and the modeling of biomolecules.

It is well established that the theoretical behavior of a material is substantially differ from its actual property. Therefore instead of using experimental route we have used computer simulations to find out theoretical tensile and ratcheting behavior of the materials. Finally, attempts have been directed to correlate the findings from simulation and the results obtained from previous experiments.

1.1 Objectives

1. To study the variation in ratcheting strain of pure aluminum with different parameters like temperature, mean stress and stress amplitude.

2. To study the variation in ratcheting strain of pure copper with different parameters like temperature, mean stress and stress amplitude.

3. To make a direct comparison between experimental data from previous research and results from simulation performed.

Chapter 2

LITERATURE REVIEW

2. Literature Review

2.1 Fatigue:

Failure of an engineering component may occur at a lower stress level than its monotonic fracture strength when it is subjected to fluctuating stresses. This failure process, called *Fatigue,* involves a gradual cracking of the component. It has become progressively more relevant in developed technology in the areas, such as automobiles, aircraft, compressors, pumps, turbines, etc., that are subjected to vibration n repeated loading. Now-a-days atleast 90 percent of mechanical failures occurs due to fatigue. The basic factors necessary to cause a fatigue failure are:

• maximum tensile stresses of sufficiently high value,
• large enough variation or fluctuation in the applied stress, and
• sufficiently large number of cycles of the applied stress.

In addition, there are a host of other variableslike stress concentration, corrosion, temperature, overload, metallurgical structure, residual stresses, and combined stresses, which tend to alter the conditions for fatigue. Though fatigue failures may seem to be sudden, the process of fatigue fracture is progressive, beginning as miniature cracks that grow during the service life of components. Sub-microscopic changes take place in the crystalline structure of metals and alloys under the action of repetitive low-level load applications. These minute changes accumulate to lead to the formation of tiny microscopic cracks. The tiny cracks grow under cyclic loading into larger cracks. The larger cracks continue to grow until the stress in the remaining ligament becomes unsustainable, when sudden failure occurs.

The growth history of fatigue cracks can conveniently be sub-divided into three stages: (i) Crack Initiation, (ii) Incremental Crack Growth, and (iii) Final Fracture.

Fatigue crack initiation usually occurs at free surfaces, because of the higher stresses and the higher probability of the existence of defects at these locations (existence of corroded or eroded areas, corrosion pits, scratches, etc.). Nevertheless, even at highly-polished defect-free surfaces, fatigue cracks can initiate through repeated micro-plastic deformations which result in the formation of the so called “intrusions” and “extrusions” on the surface. The intrusions can act as local stress concentration sites which may eventually lead to the formation of micro-cracks. The crack grows in Stage I at a slant, in a crystallographic fashion. Gradually it deflects into a Stage II crack when a striation forming mechanism dominates. Fatigue crack propagation occurs through repeated crack tip blunting and sharpening effects which are in turn caused by micro-plastic deformation mechanisms operating at the crack tip. Crack propagation occurs over a long period of time, the fracture surface may contain characteristic markings which are called “beach markings” or “clam shell markings”. These markings, which are recognizable even by naked eye, reflect the occurrence of different periods of crack growth. On the other hand, there are extremely fine parallel markings, at intervals of the order of 0.1 μm or more called “striations”, which represent the crack growth dueto individual loading cycles and can visibleunder high magnifications using electron microscopes.Striations arise via two primary mechanisms: alternating slip and crack tip blunting and resharpening.

These mechanisms are sketched below in Fig (2.1).

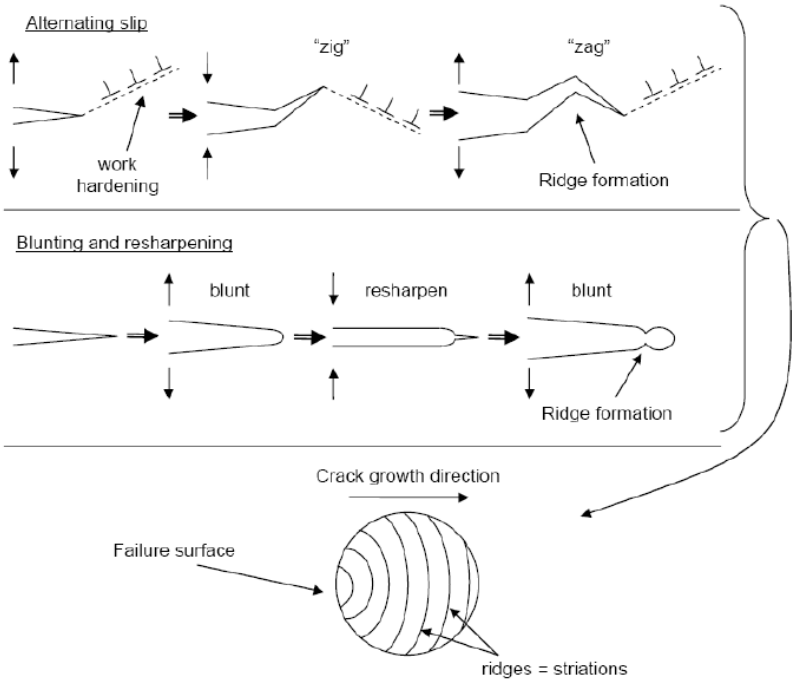

Fig 2.1. Schematic representation of mechanisms of fatigue crack growth.

Alternating slip occurs when the crack tip plasticity is limited, so that dislocations only move on a few parallel planes. As the dislocations are produced at the crack tip under load, they will tend to pile up close to the crack tip, resulting in localized work hardening. This work hardening tends to embrittle the material, making it easy for the crack to grow on the slip plane. As the crack grows, new slip planes are activated, and the process is repeated as illustrated above. As the slip planes alternate, the crack follows a "zigzag" path and sharp ridges are formed on the failure surface. Crack tip blunting and re-sharpening occurs in materials capable of more generalized yielding at the crack tip. Upon loading, the initially sharp crack will blunt due to plastic deformation. This blunting causes a small extension in the crack length. When the crack is unloaded, the elastic stress field around the plastically relaxed crack tip will cause the crack to re-sharpen. As the crack is again loaded, it again blunts, leaving behind a ripple on the surface.

Further on, in Stage III, static fracture modes are superimposed on the growth mechanism, till finally it fails catastrophically by shear at an angle to the direction of growth. Fig. 2.2 gives a schematic representation of the various stages of fatigue crack growth.

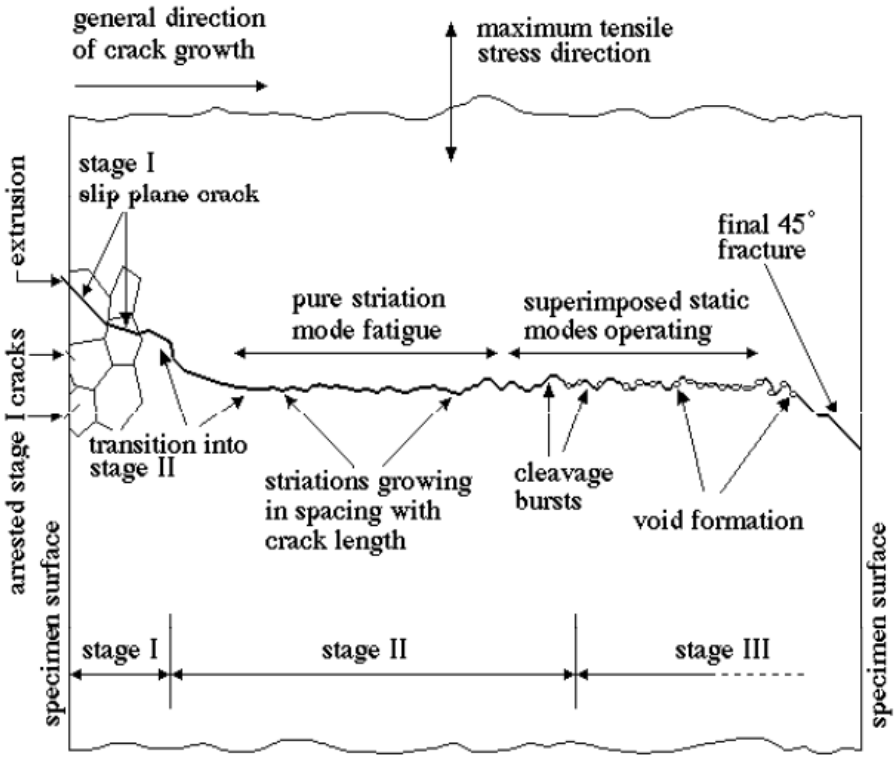

Fig 2.2. Schematic representation of the various stages of fatigue crack growth.

2.2 Stress Cycles

General types of fluctuating stress which can cause fatigue are given below:

Figure 2.3(a) illustrates completely reversed cycle of stress of sinusoidal form the Maximum and minimum stresses are equal for this type of stress cycle. In other words we can say symmetric loading ($\sigma m = 0$). Tensile stress is taken as positive and compressive stress is taken as negative.

Figure 2.3(b) illustrates a repeated stress cycle in which the maximum stress σ_{max} and σ_{min} are not equal. In this illustration both are in tension, but a repeated stress cycle could just as well contain maximum and minimum stresses of opposite signs or both in tension. This is known as asymmetric loading ($\sigma_m \neq 0$).

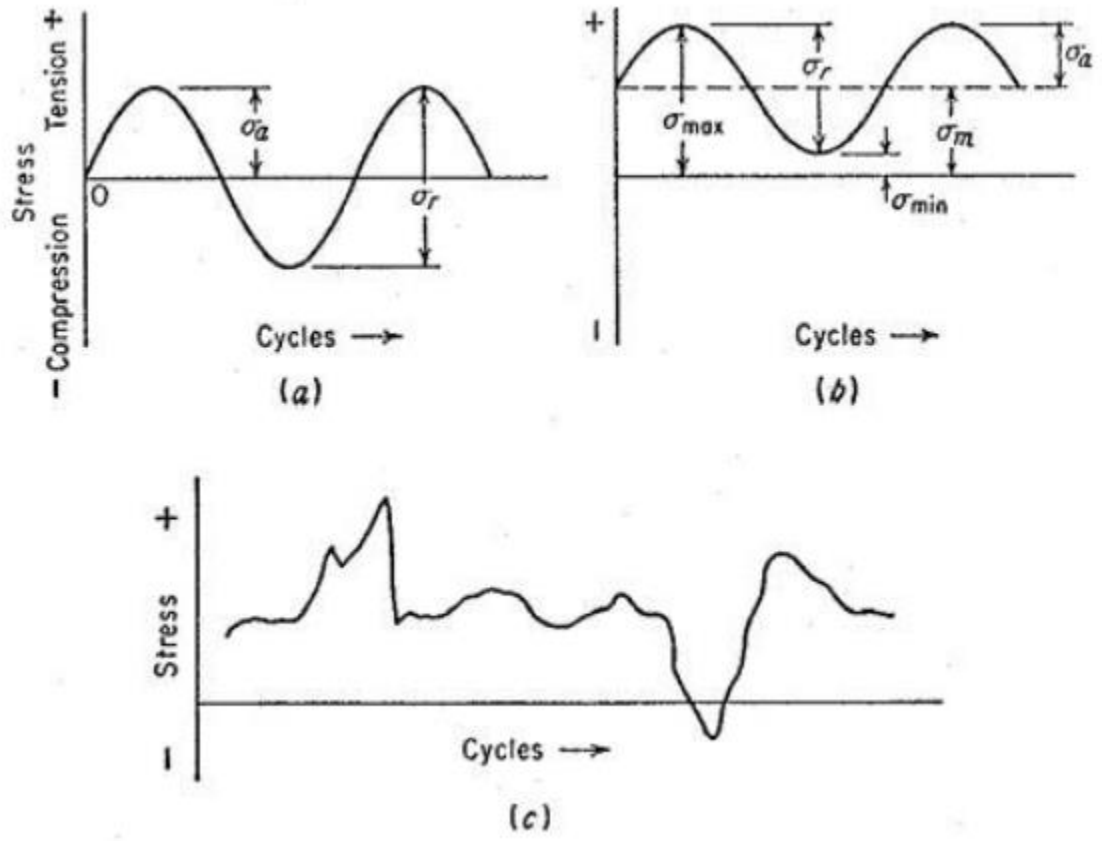

Fig. 2.3: (a) reversed stress cycle (b) repeated stress cycle (c) irregular or random stress cycle.

2.3 The S-N Curve:

The basic method of presenting engineering fatigue data is by means of the S-N curve Fig. 2.4, a plot of stress σ against the number of cycles to failure N. A log scale is almost always used for N. The value of stress that is plotted can be σ_a, σ_{max}, or σ_{min}. The stress values are usually nominal stresses, i.e., there is no adjustment for stress concentration. The S-N relationship is determined for a specified value of σ_m, R ($R=\sigma_{min}/\sigma_{max}$), or A ($A=\sigma_a/\sigma_m$).

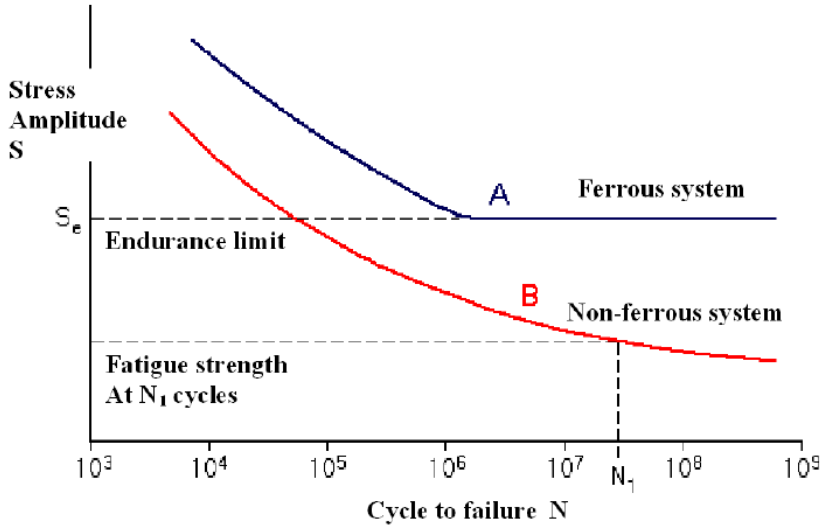

Fig. 2.4 Schematic representation of S-N curve: (A) Ferrous system; (B) Non-ferrous system

For determinations of the S-N curve, the usual procedure is to test the first specimen at a high stress where failure is expected in a fairly short number of cycles, e.g., at about two-thirds the static tensile strength of the material. The test stress is decreased for each succeeding specimen until one or two specimens do not fail in the specified numbers of cycles, which is usually at least 10^7 cycles. The highest stress at which a run-out (non-failure) is obtained is taken as the fatigue limit. For materials without a fatigue limit the test is usually terminated for practical considerations at a lowstress where the life is about 10^8 or $5x10^8$ cycles. The S-N curve is usually determined with about 8 to 12 specimens.

2.4 LCF and HCF:

Fatigue failure can be divided into two forms encompassing the total life of a component, low and high cycle fatigue (LCF and HCF). In HCF, the life is usually characterized as a function of

the stress range applied, and thecomponents fail after a high numbers(Usually higher than 10^6 cycles) of cycles at a relatively low stress(usually less than 30 % of yield stress), and the deformation experienced is primarily elastic . High cycle fatigue must be conceder during design of automobiles, aircraft, compressors, pumps, turbines, etc. where vibration occur. HCF test is done at frequency always greater than 1 KHz. From physical point of view, the repeated variation of elastic stress in metals induces micro internal stress above the local yield stress, with dissipation of energy via micro-plastic strain which arrest certain slips due to the increase of dislocations nodes. There is formation of permanent micro slip bands and de-cohesions, often at the surface of the material, to produce the mechanism of intrusion extrusion. After this stage crack located inside grain where the micro cracks follow the plane of maximum shear stress. In next stage in which the micro cracks crosses the grain boundary and grow more or less perpendicular to the direction of principal stress up to coalescence to produce a messo-crack. The opposite applies for LCF, where life is nominally characterized as a function of the strain range and the component fails after a small number of cycles at a high stress, and the deformation islargely plastic. Strain controlled cyclic loading is found in thermal cycling, where a component expands and contracts in response to fluctuations in the operating temperature. Low cycle fatigue must be considered during design of nuclear pressure vessels, steam turbines and other type of power machineries. Low cycle fatigue test is done at frequency less than 1 Hz.

2.5 Effect of Mean Stress on Fatigue:

Much of the fatigue data in the literature have been determined for conditions of completelyreversed cycles of stress, $\sigma m = 0$. However, conditions are frequently met in engineering practicewhere the stress situation consists of an alternating stress and a superimposed mean or steady stress. There are several possible methods of determining an S-N diagram for a situation where themean stress is not equal to zero. Fig. 2.5 shows the formulations that are used to take account ofmean stress in describing the fatigue endurance limit. In general, all these relationships show thatwith increase of mean stress the alternating stress amplitude required for fatigue endurance limitgradually decreases.

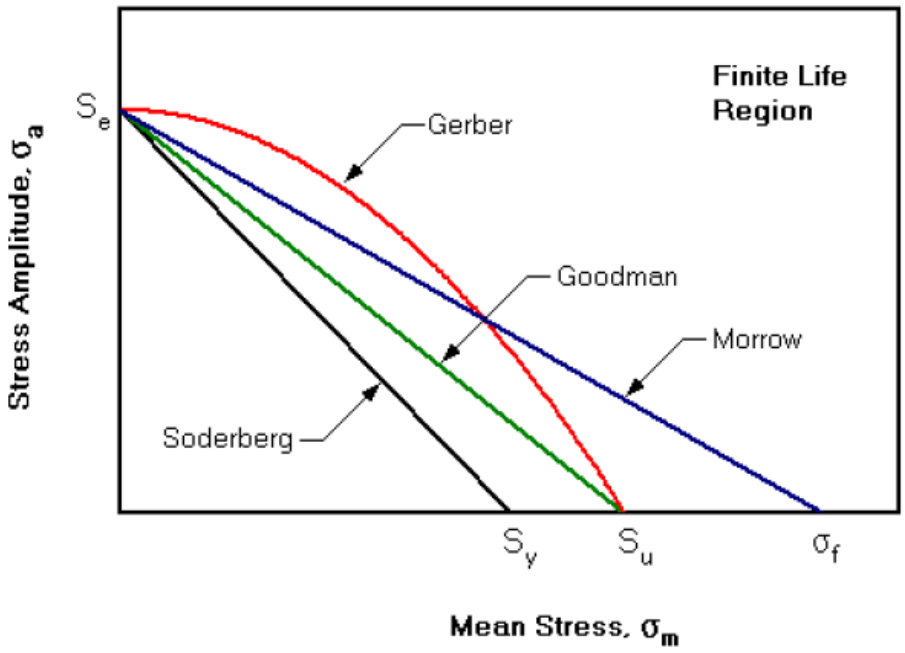

Fig.2.5. Effect of mean stress on alternating stress amplitude at fatigue endurance

The mathematical formulations for the various curves in Fig. 2.5 are:

Morrow: $(\sigma_a/\sigma_e) + (\sigma_m/\sigma_f) = 1$

Gerber : $(\sigma_a/\sigma_e) + (\sigma_m/\sigma_u)^2 = 1$

Goodman: $(\sigma_a/\sigma_e) + (\sigma_m/\sigma_u) = 1$

Soderberg: $(\sigma_a/\sigma_e) + (\sigma_m/\sigma_y) = 1$

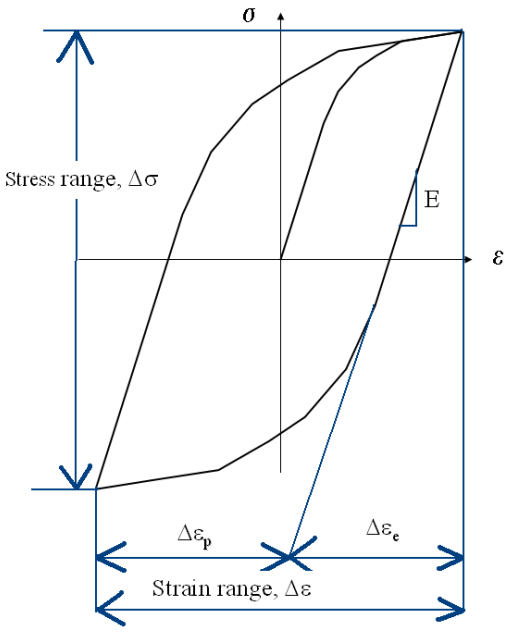

Fig 2.6. Cyclic Hysteresis Behavior

2.6 Steady state cyclic stress–strain behavior:

The hysteresis loop defined by the total strain range ($\Delta\varepsilon$) and the total stress range ($\Delta\sigma$) representsthe elastic plus plastic work on a material undergoing loading and unloading. Cyclic stress – straincurve is defined by the locus of the loop tip and has the following from the similar to the monotonic stress – strain response.

$$\varepsilon = \varepsilon_e + \varepsilon_p = \frac{\sigma_0}{E} + \left(\frac{\sigma}{k'}\right)^{\frac{1}{n'}}$$

The cyclic yield stress (σ_y) is the stress at 0.2 % plastic strain on a cyclic stress – strain curve. K' is the cyclic strength coefficient and n' is the cyclic strain-hardening exponent. Where n' represents the parameter associated with cyclic behavior, to differentiate them from those associated with monotonic behavior.

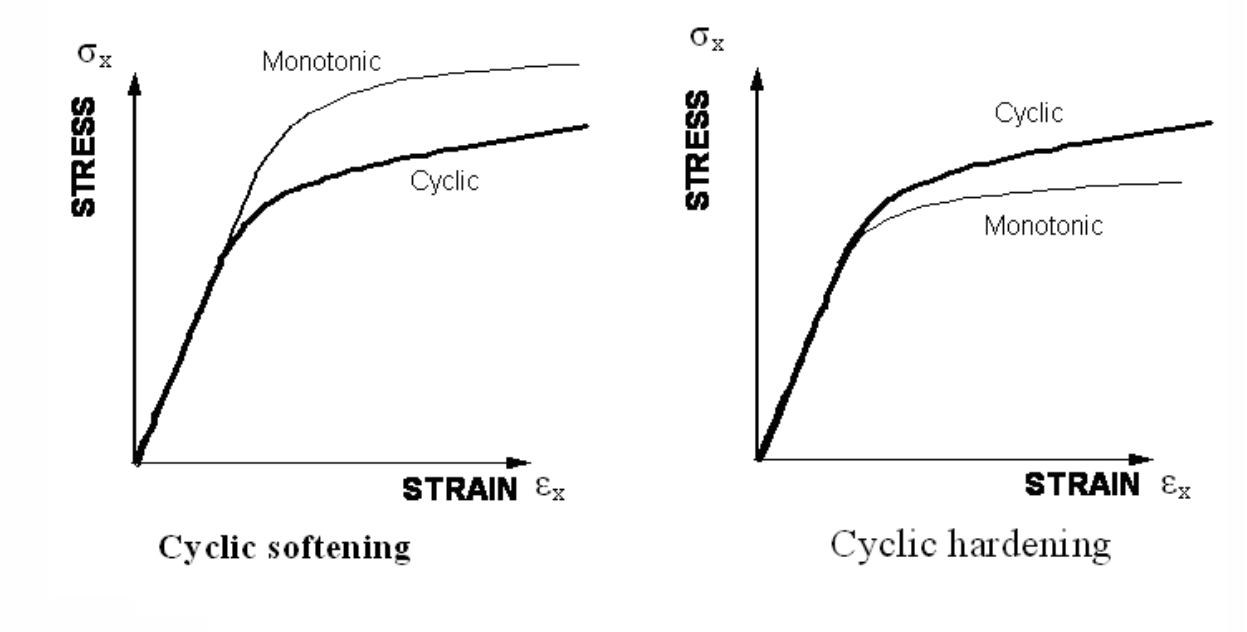

Fig 2.7 Comparison cyclic stress strain curve and monotonic stress strain curve for cyclic hardening & softening materials.

Monotonic stress strain curve is drawn from tensile test. In tensile test for a definite stress we get corresponding stain. Cyclic stress strain curve is drawn by joining tip of hysteresis loop.

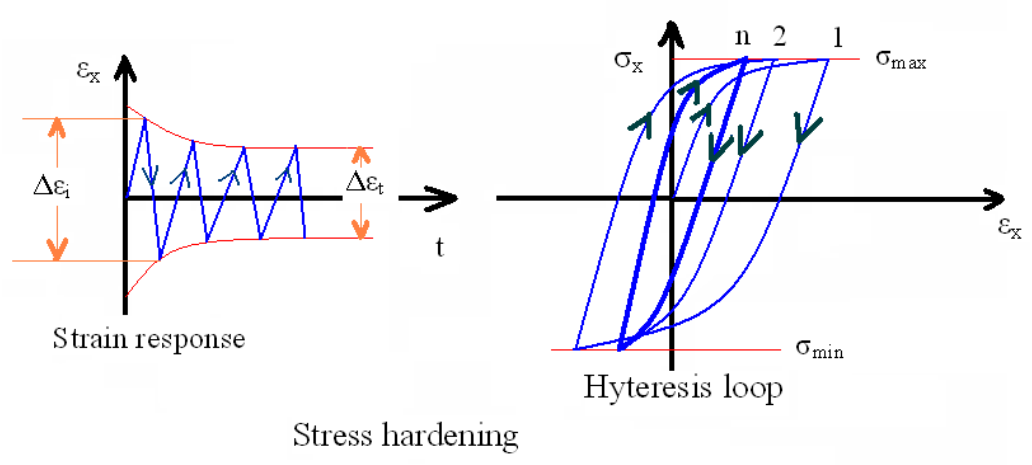

Fig. 2.8

For cyclic hardening initial strain amplitude ($\Delta\varepsilon_i$) decrease and stabilized at terminal strain amplitude ($\Delta\varepsilon_t$) in stress controlled cyclic loading. When cyclically hardening process takes place the subsequent stress strain path approach the close stable loop (n). Hardening modulus ($E_t{}^p$) is increase.

For cyclic softening initial strain amplitude ($\Delta\varepsilon_i$) increase and stabilized at terminal strain amplitude ($\Delta\varepsilon_t$) in stress controlled cyclic loading. When cyclically softening process takes place the subsequent stress strain path approach the close stable loop (n). Hardening modulus ($E_t{}^p$) is decrease.

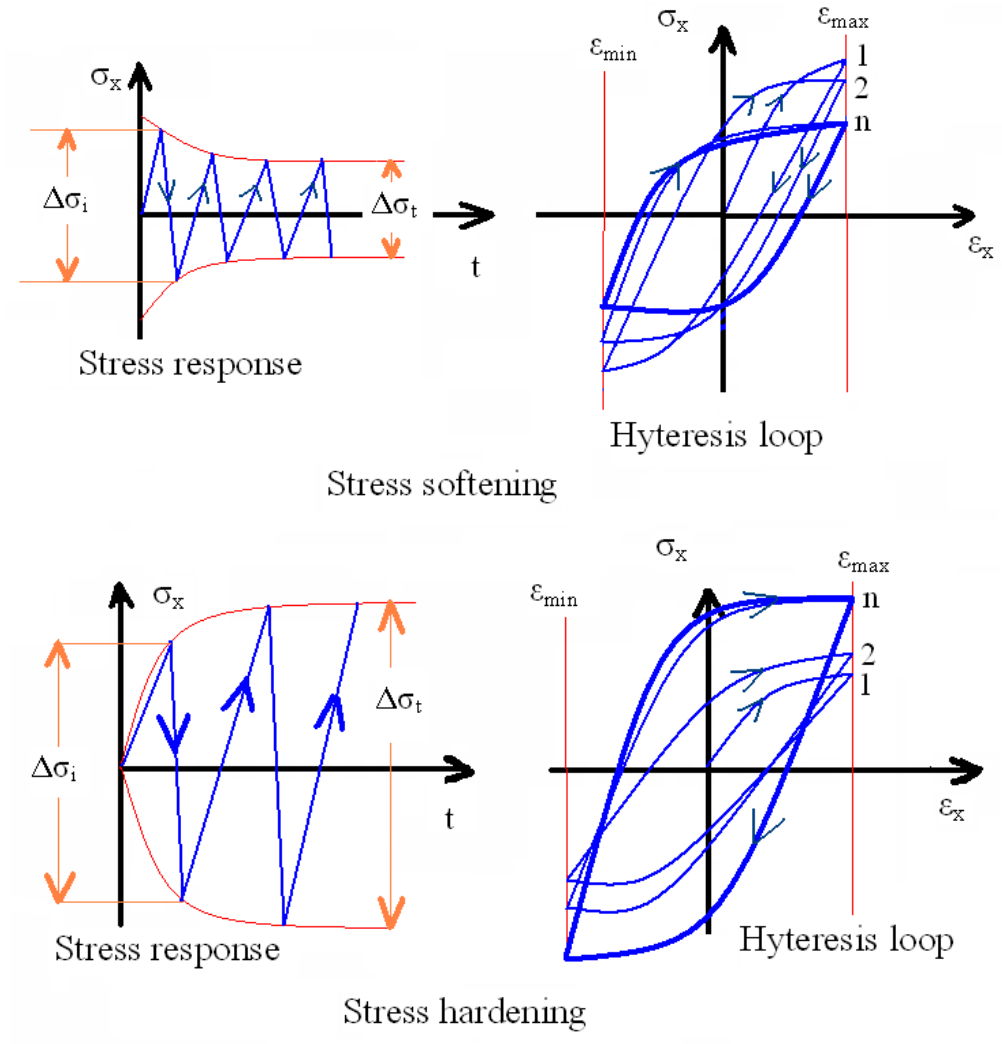

Fig 2.9 Strain controlled cyclic hardening & softening.

For cyclic hardening initial stress amplitude ($\Delta\sigma_i$) increase and stabilized at terminal stress amplitude ($\Delta\sigma_t$) in strain controlled cyclic loading. When cyclically hardening process takes place the subsequent stress strain path approach the close stable loop (n). Hardening modulus ($E_t{}^p$) is increase.

For cyclic softening initial stress amplitude ($\Delta\sigma_i$) decrease and stabilized at terminal stress amplitude ($\Delta\sigma_t$) in strain controlled cyclic loading. When cyclically softening process takes place the subsequent stress strain path approach the close stable loop (n). Hardening modulus (($E_t{}^p$) is decrease.

2.7 Ratcheting:

Ratcheting, one of the stress controlled low cycle fatigue responses, is defined as the accumulation of plastic strain with cycles. Or in other words ratcheting, a strain accumulation under stress controlled cycling with non-zero mean stress, is a predominant phenomenon in cyclic plasticity.This phenomenon is characterized by a translation of the hysteresis loop under non-symmetrical stress loading which is shown in figure below.

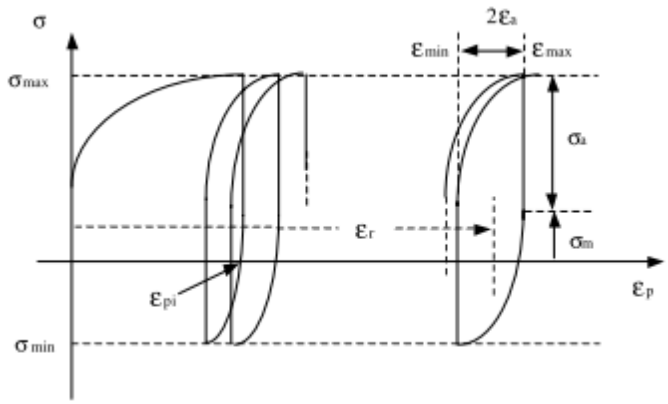

Fig 2.10 Schematic diagram for ratcheting phenomena

Ratcheting is important in designing and life evaluation of the structural components endured in cyclic loading. Ratcheting strain is a secondary strain produced under asymmetrical cyclic stressing, and has a great dependence on loading conditions and loading history. Other factors, such as ambient temperature and non-proportionality of loading path, have significant effects on ratcheting. There are different types of structures that are subjected to cyclic loading where the stress state exceeds the elastic limit of the materials used. For design and analysis of these types

of structures,accurate prediction of ratcheting response is critical as ratcheting can lead to catastrophic failure of the structures. Even for structures that are designed to be within the elastic limit, plastic zones may exist at discontinuities or at the tip of cracks. The fatigue cracks can initiate at these plastic zones. Therefore, better simulation model for cyclic plasticity response is important for the prediction of the high cycle fatigue life as well. Most metals cyclically harden or soften up to a certain number of cycles and subsequently stabilize or cease to change the size of the yield surface. Ratcheting, though, keeps on occurring with cycle seven after the material stabilizes. Hence, the kinematic hardening (translation of the yield surface in stress space) is attributed to be the primary reason for ratcheting. The axial ratcheting strain ε_r is defined as fig. 2.10

$$\varepsilon_r = \frac{1}{2}(\varepsilon_{min} + \varepsilon_{max})$$

Where ε_{max} is the maximum of axial strain is in each cycle, ε_{min} is the minimum axial strain. The axial Ratcheting strain rate is defined as the increment of ratcheting strain ε_r in each cycle and denoted as $d\varepsilon_r/dN$.

The axial ratcheting strain ε_r and torsional ratcheting strain εr are defined as following for uniaxial and multi axial stress cycling:

$$\varepsilon_r = \frac{1}{2}(\varepsilon_{min} + \varepsilon_{max})$$

$$\gamma_r = \frac{1}{2}(\gamma_{min} + \gamma_{max})$$

Where ε_{max} & γ_{max} are the maximum of axial and torsional strain in each cycle, and ε_{min} & γ_{min} are the minimum, respectively. Ratcheting strain rates are defined as $d\varepsilon_r/dN$ and $d\gamma_r/dN$ i.e. the increment of ratcheting strain ε_r and γ_r in each cycle. The values of ε_{min}, ε_{max}, γ_{min} and γ_{max} in each cycle under asymmetrical stress cycling were obtained from the collected experimental data. Thus the ratcheting strains ε_r and γ_r were calculated.

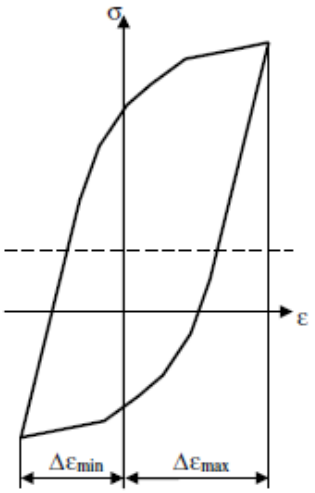

Fig 2.11.Peak stress and strain.

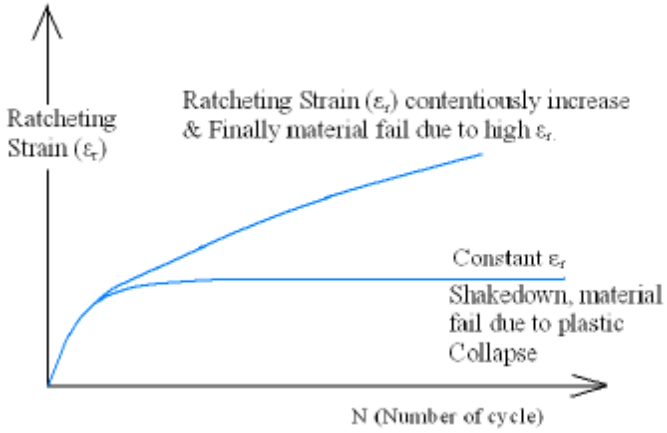

Fig 2.12 .Plot of ratcheting strain εr vs. number of cycle (N).

In the above fig (2.12) we plot ratcheting strain ε_rVs number of cycle (N). If ratcheting strain $\varepsilon_r$increase continuously with number of cycle (N) that indicates, plastic strain accumulated with time and material is finally failed due to high plastic strain. If ratcheting strain $\varepsilon_r$first increase with number of cycle (N) then comes to a constant value that indicates that in first portion of the curve plastic strain accumulated with time then stops, so material don't fail due to ratcheting.

2.8 Effect of mean stress and stress amplitude

In true stress controlled fatigue test S. K. Paul et. al [26] found ratcheting strain varies directly with the stress amplitude at constant mean stress, which is explained by the graph shown below. In case of constant stress amplitude both ratcheting life and strain accumulation is increasing

with tensile mean stress and strain accumulation paths are mirror of each other for tensile and compressive mean stress of equal magnitude. G. Chen et. al [27] concluded that ratcheting strain amplitude and ratcheting strain rate of 63Sn37Pb increased with increasing stress amplitude or mean stress correspondingly and also showed that ratcheting strain rate was very sensitive to the applied cyclic stress rate. Several other researchers have found that ratcheting strain depends on both mean stress and stress amplitude.

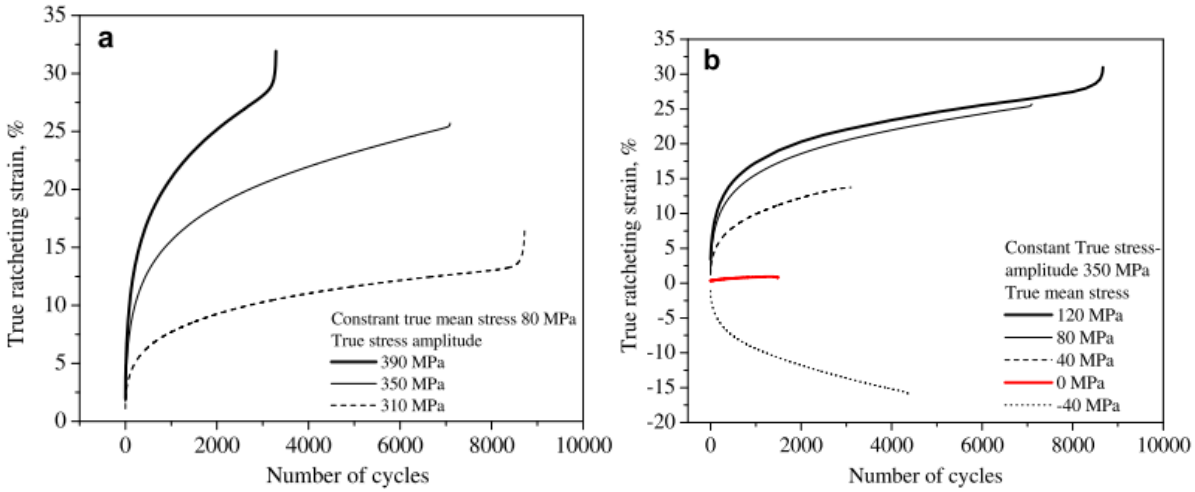

True ratcheting Strain versus number of cycles: (a) constant σm: 80 MPa and σa: 310, 350 and 390 MPa (b) constant σa= 350 MPa and σm: -40, 0, 40, 80 and 120 MPa.

2.9 Molecular dynamics simulation

Molecular dynamics (MD) is a computer based simulation of physical movements of molecules and atoms. The atoms and molecules are then allowed to interact for a period of time, which gives a view of the motion of the atoms. Commonly, the trajectories of molecules and atoms are determined by solving the Newton's motion equations for a system of interacting particles, where forces among particles and potential energy are defined by force fields of molecular mechanics. Originally this method was conceived within theoretical physics during 1950 to 1960, but is applied today mostly in materials science and biomolecules modeling.

The results of these simulations may be used to determine macroscopic thermodynamic properties of the system as per the ergodic hypothesis: the statistical ensemble averages and the time averages of the system are equal. MD has also been known as "statistical mechanics by

numbers" and "Laplace's vision of Newtonian mechanics" of predicting the future by animating nature's forces and providing an insight into molecular motion on an atomic scale.

The obvious advantage of MD is that it gives an idea of dynamical properties of the system: transport coefficients, time-dependent responses to perturbations, rheological properties and spectra.

2.10 Areas of Application

In chemistry and biophysics, the interaction between the particles is either explained by a "force field" (classical MD), a quantum chemical model, or a mixture of the two. These terms are not used in physics, where interactions are usually described by name of the theory or approximation used and called the potential energy, or simply “potential".

Beginning in theoretical physics, the MD method gained popularity in materials science and also in biochemistry and biophysics since 1970s. In chemistry, MD serves as an important tool in determining and refining of protein structure using experimental tools such as X-ray crystallography and NMR. It is also applied with limited success in refining protein structure predictions. MD in physics is used to examine the atomic-level dynamics that cannot be observed directly, such as thin film growth and ion-sub plantation. It is also used to examine the physical properties of Nano technological devices that have not or cannot yet be created.

Molecular dynamics, in applied mathematics and theoretical physics, is a part of the research area of dynamical systems, ergodic theory, Atomic, molecular, and optical physics and statistical mechanics in general. The concepts of molecular entropy and energy conservation come from thermodynamics. Some techniques like principal components analysiscome from information theoryto calculate conformational entropy. Mathematical techniques like the transfer operator are applicable when MD is considered as a Markov chain.

MD can also be considered as a case of discrete element method (DEM) where the particles have spherical shape (e.g. with the size of their van der Waals radii.)

2.11 Design constraints

A molecular dynamics simulation should be so designed that it should account for the available computational power. Simulation size (n=number of particles), timestep and total time duration

must be selected so that the calculation can finish within a reasonable time period. However, the simulations ought to be long enough for it to be relevant to the time scales of the natural processes which are being studied. The time span of the simulation should match the kinetics of the natural process for it to make statistically valid conclusions. Most scientific publications about the dynamics of proteins and DNA use data from simulations varying from nanoseconds (10−9 s) to microseconds (10−6 s). The time span of these simulations varies from several CPU-days to CPU-years. Parallel algorithms like spatial or force decomposition algorithm allow the load to be distributed among CPUs.

During a classical MD simulation, the most CPU intensive task is the evaluation of the potential (force field) as a function of the particles' internal coordinates. The non-bonded or non-covalent part of energy evaluation is the most expensive one. In Big O notation, common molecular dynamics simulations scale by O(n2) if all pair-wise electrostatic and van der Waals interactions must be accounted for explicitly. This computational cost can be reduced by employing electrostatics methods such as Particle Mesh Ewald (O(n(log(n)), P3M or good spherical cut off techniques (O(n)).

Another major factor that impacts total CPU time required for a simulation is, size of the integration timestep. It is the time duration between evaluations of the potential. The timestep must be small enough to avoid discretization errors (i.e. smaller than the frequency of fastest vibrations of the system). Typical timesteps for classical MD are in the order of 1 femtosecond (10−15 s). Algorithms like the SHAKE can extend this value as they fix the vibrations of the fastest atoms (e.g. hydrogen) into place.

For simulating molecules in a solvent, a choice should be made between explicit solvent and implicit solvent. Explicit solvent particles (such as the TIP3P, SPC/E and SPC-f water models) must be calculated expensively by the force field, while implicit solvents use a mean-field approach. Use of an explicit solvent is computationally expensive as it requires inclusion of roughly ten times more particles in the simulation. But the granularity and viscosity of explicit solvent is necessary to generate certain properties of the solute molecules. This is especially important to generate kinetics.

The simulation box size, in all kinds of molecular dynamics simulations, must be large enough to avoid boundary condition artifacts. Boundary conditions are often treated by choosing fixed

values at the edges (which may cause artifacts), or by employing periodic boundary conditions in which one side of the simulation loops back to the opposite side, imitating a bulk phase.

Microcanonical ensemble (NVE)

In the microcanonical, or NVE ensemble, the system is isolated from changes in moles (N), volume (V) and energy (E). It is an adiabatic process with no heat transfer involved. A microcanonical molecular dynamics trajectory can be said to be an exchange of potential and kinetic energy keeping total energy conserved. For a system of N particles with coordinates X and velocities V, the following pair of first order differential equations may be written in Newton's notation as

$$F(X) = -\nabla U(X) = M\,\dot{V}(t)$$

$$V(t) = \dot{X}(t)$$

The potential energy function U(X) of the system is a function of the particle coordinates X. It is referred to simply as the "potential" in physics, or the "force field" in chemistry. The first equation comes from Newton's laws; the force 'F' acting on each particle in the system can be calculated as the negative gradient of U(X).

For every timestep, each particle's position X and velocity V can be integrated with a symplectic method like Verlet. Time evolution of X and V is called a trajectory. Given the initial positions, from theoretical knowledge, and velocities ,from randomized Gaussian, we can calculate all future (or past) positions and velocities.

The meaning of temperature in MD is one frequent source of confusion. Commonly we have experience with macroscopic temperatures involving a huge number of particles. But temperature is statistical in nature. If there is a large enough number of atoms, statistical temperature can be estimated from the instantaneous temperature, which is found by equating the kinetic energy of the system to nkBT/2 where n is the number of degrees of freedom of the system.

The temperature of the system in NVE is rises naturally when macromolecules such as proteins undergo exothermic conformational changes and binding.

Canonical ensemble (NVT)

In the canonical ensemble, moles (N), volume (V) and temperature (T) are conserved and is also sometimes called as constant temperature molecular dynamics (CTMD). In NVT, the energy of endothermic and exothermic processes is exchanged with a thermostat.

A variety of thermostat methods is available to add and remove energy from the boundaries of an MD system in a more or less realistic way, approximating the canonical ensemble. Popular techniques to control temperature include velocity rescaling, the Nosé-Hoover thermostat, Nosé-Hoover chains, the Berendsen thermostat and Langevin dynamics.

Isothermal–isobaric (NPT) ensemble

In the isothermal–isobaric ensemble, moles (N), pressure (P) and temperature (T) are conserved. Along with a thermostat, a barostat is also needed. It corresponds to laboratory conditions with a flask open to ambient temperature and pressure.

In the simulation of biological membranes, isotropic pressure control is inappropriate. For lipid bilayers, pressure control occurs under constant membrane area (NPAT) or constant surface tension "gamma" (NPγT).

Generalized ensembles

The replica exchange method is a generalized ensemble. Originally created to deal with the slow dynamics of disordered spin systems, also called parallel tempering, is a replica exchange MD (REMD) formulation[12] tries to overcome the multiple-minima problem by exchanging the temperature of non-interacting replicas of the system running at several temperatures.

2.12 Potentials in MD simulations

A molecular dynamics simulation requires a description of the particles in the simulation will interact. It is also referred to as a force field in chemistry and biology. Potentials may be defined at many levels of physical accuracy; those most commonly used in chemistry are based on molecular mechanics and personify a classical treatment of particle-particle interactions that can generate structural and conformational changes but usually cannot produce chemical reactions.

The reduction from a quantum description to a classical potential two approximations is needed. The first one is the Born–Oppenheimer approximation, which states that the dynamics of electrons is so fast that they can be considered to react instantaneously to the motion of their nuclei. So they may be treated separately. The second one treats the nuclei, much heavier than electrons, as point particles that follow classical Newtonian dynamics. In classical molecular dynamics the effect of the electrons is approximated as a single potential energy surface representing the ground state usually.

When finer levels of detail are required, potentials based on quantum mechanics are used; some techniques attempt to create hybrid classical/quantum potentials where the bulk of the system is treated classically but a small region is treated as a quantum system which usually undergoes a chemical transformation.

2.13 Empirical potentials

Empirical potentials used in chemistry are frequently called force fields, while those used in materials physics are called just empirical or analytical potentials. Most force fields in chemistry are empirical and consist of a summation of bonded forces associated with chemical bonds, bond angles, and bond dihedrals, and non-bonded forces associated with van der Waals forces and electrostatic charge. Empirical potentials represent quantum-mechanical effects in a limited way through ad-hoc functional approximations. These potentials contain free parameters such as atomic charge, van der Waals parameters reflecting estimates of atomic radius, and equilibrium bond length, angle, and dihedral; these are obtained by fitting against detailed electronic calculations (quantum chemical simulations) or experimental physical properties such as elastic constants, lattice parameters and spectroscopic measurements.

Because of the non-local nature of non-bonded interactions, they involve at least weak interactions between all particles in the system. Its calculation is normally the bottleneck in the speed of MD simulations. To lower the computational cost, force fields employ numerical approximations such as shifted cutoff radii, reaction field algorithms, particle mesh Ewald summation, or the newer Particle-Particle Particle Mesh (P3M).

Chemistry force fields commonly employ preset bonding arrangements (an exception being *ab initio* dynamics), and thus are unable to model the process of chemical bond breaking and reactions explicitly. On the other hand, many of the potentials used in physics, such as those based on the bond order formalism can describe several different coordinates of a system and bond breaking. Examples of such potentials include the Brenner potential for hydrocarbons and its further developments for the C-Si-H and C-O-H systems. The ReaxFF potential can be considered a fully reactive hybrid between bond order potentials and chemistry force fields.

Because molecular systems consist of a vast number of particles, it is impossible to find the properties of such complex systems analytically; MD simulation circumvents this problem by using numerical methods. However, long MD simulations are mathematically ill-conditioned, generating cumulative errors in numerical integration that can be minimized with proper selection of algorithms and parameters, but not eliminated entirely.

In this investigation, LAMMPS is the software used for simulation. It is a molecular dynamics program from Sandia National Laboratories. LAMMPS is a classical molecular dynamics code, and an acronym for Large-scale Atomic/Molecular Massively Parallel Simulator. LAMMPS has potentials for soft materials (biomolecules, polymers) and solid-state materials (metals, semiconductors) and coarse-grained or mesoscopic systems. It can be used to model atoms or, more generically, as a parallel particle simulator at the atomic, meso, or continuum scale. LAMMPS runs on single processors or in parallel using message-passing techniques and a spatial-decomposition of the simulation domain. The code is designed to be easy to modify or extend with new functionality.

Chapter 3

SIMULATION PARAMETERS

3. SIMULATION PARAMETERS

Reason for using Molecular Dynamics Simulation

Experimental fatigue tests have already been done with copper but testing using Molecular Dynamics simulation has not been done yet. Use of MD simulation gives the advantage of 100% pure copper which is practically not possible to get. Moreover using this route we can do the tests in sub-ambient, ambient and elevated temperatures and these facilities are not available in our labs. Using this technique time consuming fatigue experiments can be done in few hours.

While writing the simulation input file code, variables like potential file, lattice parameters, maximum and minimum stress, temperature, number of cycles and number of iterations are changed. These are the parameters which govern the simulation conditions and environment, and they are the simulation parameters.

Stress values for practical experiments are much lesser than that required for simulations. This is because practical cohesive strength is lower than ultimate tensile strength. This is explained by Griffith's criterion. While simulating, we take 100% pure sample but practically attaining 100% purity is not possible. These imperfections and micro-cracks acts as regions of high stress concentrations where failure occurs at much lower levels of applied stresses.

3.1 FATIGUE TESTING:

In order to find the variation of ratcheting strain we are doing low cycle fatigue testing of pure copper and pure aluminum. In low cycle fatigue experiments the value of applied stress is above the yield stress of the material but lower than its ultimate tensile strength. Values of mean stress and alternate stresses are chosen decisively. Testing is done at three values of mean stress and three values of alternate stress. Therefore we can represent the stress parameters in the form of a 9X9 matrix.

3.2 To find the variation of ratcheting strain with varying mean stress and alternate stress

3.2.1 Copper

Yield strength= 70MPa Ultimate tensile strength= 210MPa [ASM Handbook]

Test matrix for practical experiments

Stress amplitude (in MPa)	Mean stress = 10MPa	Mean stress = 20MPa	Mean stress = 30MPa
120	σ_{max} = 130 σ_{min} = -110	σ_{max} = 140 σ_{min} = -100	σ_{max} = 150 σ_{min} = -90
140	σ_{max} = 150 σ_{min} = -130	σ_{max} = 160 σ_{min} = -120	σ_{max} = 170 σ_{min} = -110
160	σ_{max} = 170 σ_{min} = -150	σ_{max} = 180 σ_{min} = -140	σ_{max} = 190 σ_{min} = -130

Values of stresses are in MPa

Practically Copper breaks at 210MPa (from ASM Handbook) but while simulation the material withstood stress values as high as 16500MPa, i.e. 80 times higher value. Therefore test matrix is multiplied by 80 to get the simulation matrix.

Test matrix for simulation

Test matrix (9X9simulations) is to find variation of ratcheting strain with varying mean stress and stress amplitude.

Stress amplitude (in MPa)	Mean stress = 800MPa	Mean stress = 1600MPa	Mean stress = 2400MPa
9400	σ_{max} = 10250 σ_{min} = -8635	σ_{max} = 10990 σ_{min} = -7850	σ_{max} = 11775 σ_{min} = -7065
11000	σ_{max} =11775 σ_{min} = -10250	σ_{max} = 12560 σ_{min} = -9420	σ_{max} = 13345 σ_{min} = -8635

12600	σ_{max} = 13345 σ_{min} = -11775	σ_{max} = 14130 σ_{min} = -10990	σ_{max} = 14915 σ_{min} = -10250

Values of stresses are in MPa

3.2.1.1 Input file for simulation of fatigue test on Pure Copper of box size [20 50 20]

```
# This program is for tensile-fatigue testing of pure Cu

unitsmetal
echo           both
atom_style     atomic
dimension      3
boundary       p p p
regionbox block 0 20 0 50 0 20  units box
create_box      1 box
lattice         fcc 3.61-----→ Lattice type and Lattice parameter
regionCu block   0 20 0 50  0 20 units box→ define box size( xlo xhi ylo yhi zlo zhi)
create_atoms1 region Cu units box

timestep0.002
pair_styleeam/fs
pair_coeff     * * Cu_zhou.eam.alloy Cu→ Potential FileName

# mobile zone

region        1 block 0 20 0 10 0 20 units box
region        2 block 0 20 40 50 0 20 units box

group            lower region 1
group            upper region 2
group            boundary union lower upper
group            mobile subtract all boundary


# Energy Minimization
minimize         1.0e-4 1.0e-7 10000 100000

#output
compute         2   mobile temp
thermo          100
thermo_style  custom step temp ylo yhi press etotal pyy c_2

dump 2 all atom 1000 Cu_fatigue_LOOP_300k_2,1.dump.lammpstrj
dump_modify 2 scale no
log logCu_fatigue_3d_LOOP_300k_2,1.data

dump  3 mobile atom 1000 Cu_fatigue_mobile_LOOP_300k_2,1.dump.lammpstrj
dump_modify   3 scale no


# initializing velocities

velocity     mobile create 300.0 873847 rot yes mom yes distgaussian
```

```
#compute:structure

compute       myRDF all rdf 100
fix           1  all ave/time 1000 1 1000 c_myRDF file
Cu_fatigue_mobile_LOOP_300k_2,1.rdf mode vector


#fixes

fix                 2 boundary setforce 0.0 0.0 0.0

#fix                3 mobile nvt temp 300 300 100
fix3 mobile nve
fix4 mobile temp/rescale 100 300 300 0.05 1.0
                                                    (starting T ending T)

# loop is given below for d fixes 5,6,7,8

label       loop1
# to generate loops change from here
variable     d loop 20
label  loopstart
# number of cycles
variable      a loop 4
variable      s index     0     -152000          0     104000
variable      e index   -152000     0          104000     0
fix          5 mobile press/berendsen y $s $e 100 dilate all
run           10000
#log log.$s-$e
next          s
next          e
next          a
jump          in.Cu_fatigue_loop_Danloopstart
next d

jump          in.Cu_fatigue_loop_Dan loop1
```

→ **temperature**

→ **enter the no. of cycles here**

→ **stress range is mentioned here**

→ **number of iterations**

3.2.2 Aluminum

Yield strength = 95MPa Ultimate Tensile Strength = 110MPa [ASM Handbook]

Test matrix for practical experiments

Alternate stress (in MPa)	Mean stress = 4 MPa	Mean stress = 8 MPa	Mean stress = 12 MPa
85	σ_{max} = 89 σ_{min} = -81	σ_{max} = 93 σ_{min} = -77	σ_{max} = 97 σ_{min} = -73
90	σ_{max} = 94 σ_{min} = -86	σ_{max} = 98 σ_{min} = -82	σ_{max} = 102 σ_{min} = -78

95	σ_{max} = 99 σ_{min} = -91	σ_{max} = 103 σ_{min} = -87	σ_{max} = 107 σ_{min} = -83

Values of stresses are in MPa

Practically Aluminum fails at 110MPa (from ASM Handbook) but while simulation the material withstood stress values as high as 9900MPa, i.e. 90 times higher value. Therefore test matrix is multiplied by 90 to get the simulation matrix.

Test matrix for simulation

Alternate stress (in MPa)	Mean stress = 360MPa	Mean stress = 720MPa	Mean stress = 1080MPa
7650	σ_{max} =8010 σ_{min} = -7290	σ_{max} =8370 σ_{min} = -6930	σ_{max} =8730 σ_{min} = - 6570
8100	σ_{max} =8460 σ_{min} = -7740	σ_{max} =8820 σ_{min} = -7380	σ_{max} =9180 σ_{min} = -7020
8550	σ_{max} =8910 σ_{min} = -8190	σ_{max} =9270 σ_{min} = -7830	σ_{max} =9630 σ_{min} = -7470

Values of stresses are in MPa

Input file for simulation of fatigue test on Pure Aluminum of box size [20 50 20]

```
# This program is for tensile-fatigue testing of pure Al

units           metal
echo         both
atom_style      atomic
dimension    3
boundary        p pp
region          box block 0 20 0 50 0 20  units box
create_box      1 box

lattice      fcc 4.04
region          Al block 0 20 0 50  0 20 units box
create_atoms    1 region Al units box

timestep        0.002
pair_styleeam/fs
pair_coeff      * * Al_mm.eam.fs Al

# mobile zone
```

```
region       1 block 0 20 0 10 0 20 units box
region       2 block 0 20 40 50 0 20 units box

group           lower region 1
group           upper region 2
group           boundary union lower upper
group           mobile subtract all boundary


# Energy Minimization
minimize        1.0e-4 1.0e-7 10000 100000

#output
compute2   mobile temp
thermo100
thermo_stylecustom step temp yloyhietotal press pyy c_2

dump2 all atom 1000 Al_fatigue_LOOP_300k_2,1.dump.lammpstrj
dump_modify2 scale no
log logAl_fatigue_3d_LOOP_300k_2,1.data

dump3 mobile atom 1000 Al_fatigue_mobile_LOOP_300k_2,1.dump.lammpstrj
dump_modify3 scale no


# initializing velocities

velocitymobile create 300.0 873847 rot yes mom yes distgaussian

#compute:structure

computemyRDF all rdf 100
fix1  all ave/time 1000 1 1000 c_myRDF file Al_fatigue_mobile_LOOP_300k_2,1.rdf mode
vector


#fixes

fix          2 boundary setforce 0.0 0.0 0.0

#fix              3 mobile nvt temp 300 300 100
fix3 mobile nve
fix4 mobile temp/rescale 100 300 300 0.05 1.0


fix11 mobile npt temp 300 300 0.1 iso 0.0 0.0 0.2

run10000
unfix11



# loop is given below for d fixes 5,6,7,8

label      loop1
# to generate loops change from here
variable    d loop 10
label  loopstart
# number of cycles
variable     a loop 4
variable     s index     0    -80100          0    72900
variable     e index   -80100     0          72900    0
fix         5 mobile press/berendsen y $s $e 100 dilate all
run          10000
```

```
#log log.$s-$e
next          s
next          e
next          a
jump          in.Al_fatigue_loop_Danloopstart
nextd

jump          in.Al_fatigue_loop_Dan loop1
```

From the results obtained from simulations, two sets of graphs were plotted. One keeping means stress constant and varying alternate stress, other with varying mean stress and constant mean stress.

3.4 Fatigue testing to find the variation of ratcheting strain with varying temperature

In order to find the effect of temperature on the ratcheting behavior simulations were carried out at a range of temperature below the melting point of the material.

Melting point of copper is 1080^{o}C(1353K), therefore fatigue simulations were carried out at 200K(Sub-zero test), 300K(Room temperature), 500K and 700K in a stress range of [12600MPa, -10400MPa]. Similarly, melting point of aluminum is 660^{o}C, therefore fatigue simulation were carried out at temperatures: 200K(Sub-zero test), 300K(Room temperature), 400K and 500K in a stress range of [8460MPa,-7740MPa].

Finally, separate graphs were plotted for Copper and Aluminum showing the variation of ratcheting strain with temperature.

CHAPTER 4

RESULTS AND DISCUSSION

4.1 Ratcheting behavior: Nature of hysteresis loops:

It is well-known that hysteresis loops those are generated during ratcheting experiments gets shifted towards positive plastic loading direction under application of positive mean stress. Typical stress-strain hysteresis loops for aluminum is given in Fig. 4.1(a), and its enlarged view is given in Fig. 4.1(b). Similar hysteresis loops for copper is presented in Fig. 4.2(a), and its enlarged view is given in Fig. 4.2(b). Strain accumulation in a particular cycle is not very large, and hence the hysteresis loops in its original form are not distinguishable. It can be noted here hysteresis loops generated from all other experiments are of similar nature.

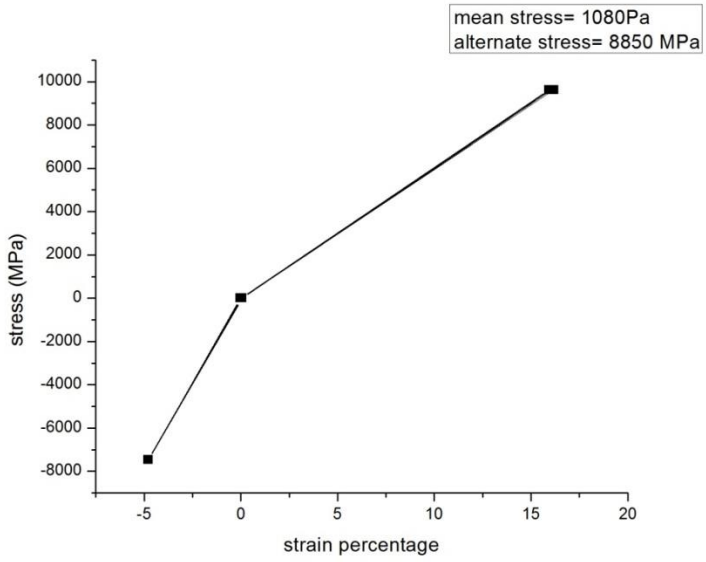

Hysteresis Loops
For Aluminum

Fig. 4.1(a)

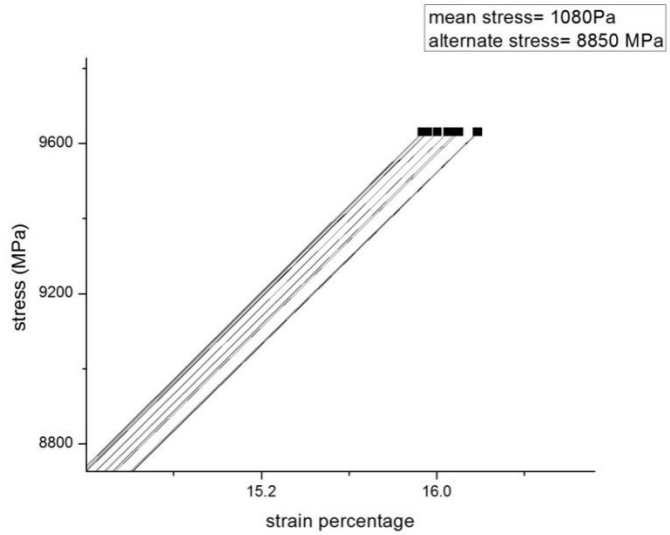

Enlarged version of the progressive hysteresis loop showing ratcheting strain

Fig. 4.1(b)

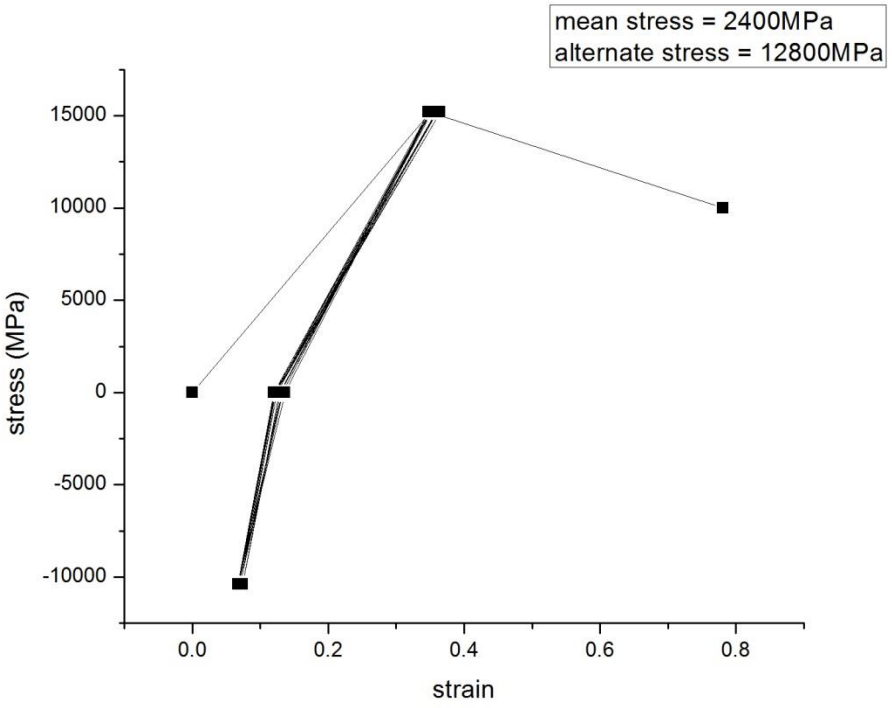

Hysteresis Loops
For Copper

Fig. 4.2(a)

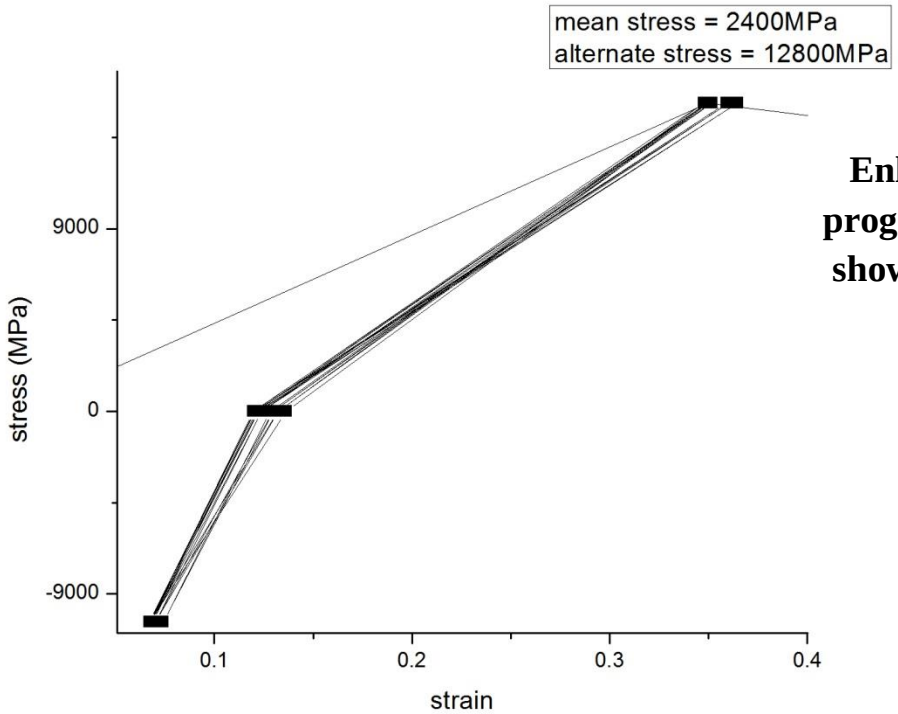

Enlarged version of the progressive hysteresis loop showing ratcheting strain

Fig. 4.2(b)

4.2 Strain accumulation under varying stress amplitude at constant mean stress:

Aluminum

The nature of variations of ratcheting strain which is getting accumulated in cyclic loading with increasing number of cycles for varying alternate stress at constant mean stress levels of 360, 720 and 1080 MPa are shown in Fig. 4.3 – Fig. 4.5. The results in these figures indicate that ratcheting strain ε_r increases quickly in the initial cycle, after which it almost negligibly increases in magnitude. This nature of strain increment was found for all the investigated stress combinations. It can also be stated that at a constant mean stress and at any specific N value, the magnitude of total accumulated ratcheting strain increases with increasing stress amplitude. All the investigated cyclic loading tests of Aluminum are up to ten cycles.

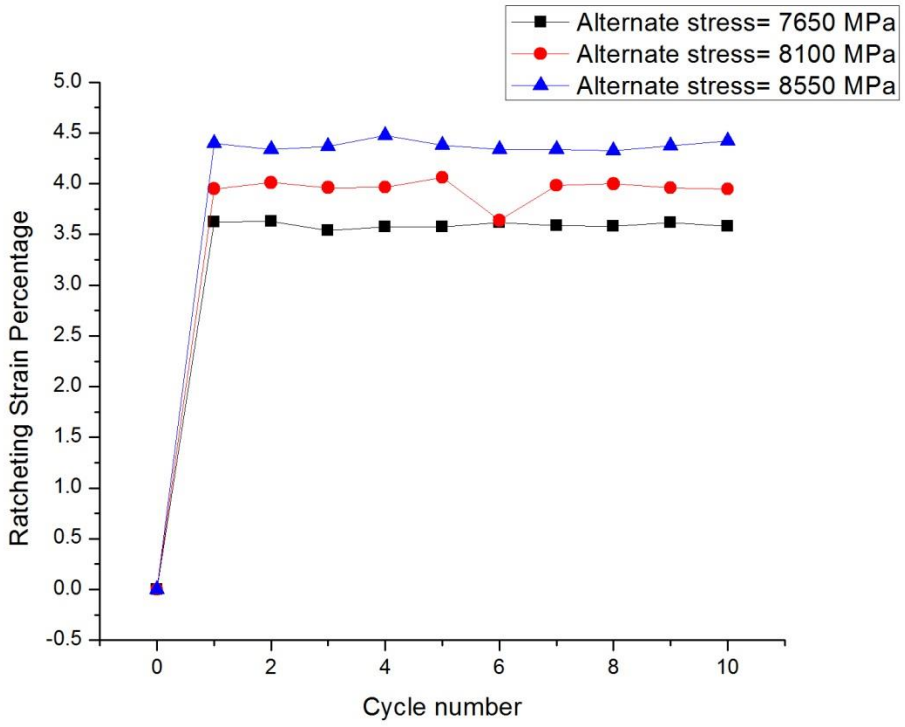

Mean stress = 360MPa
Fig. 4.3

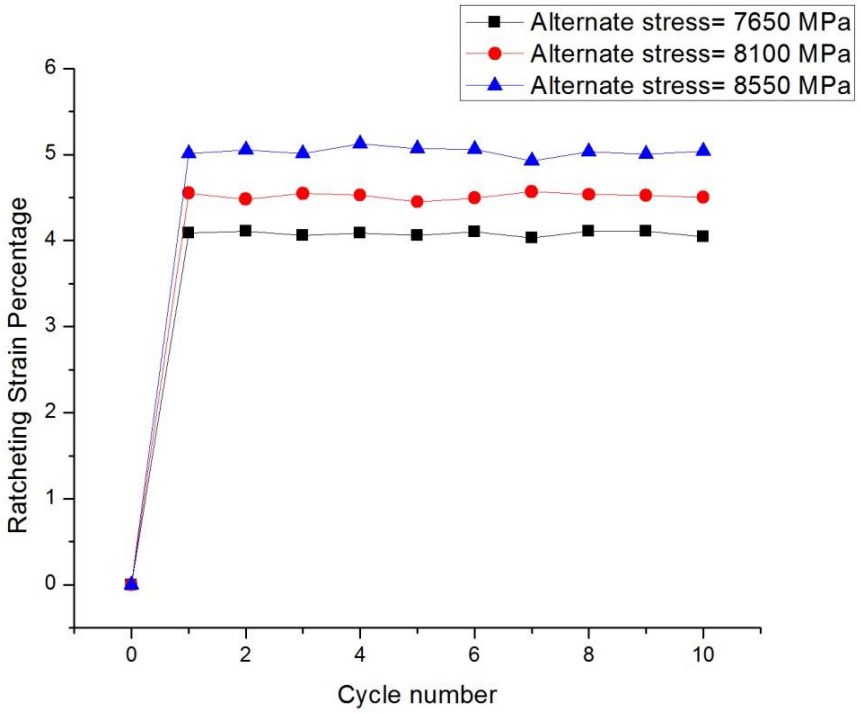

Mean stress = 720MPa
Fig. 4.4

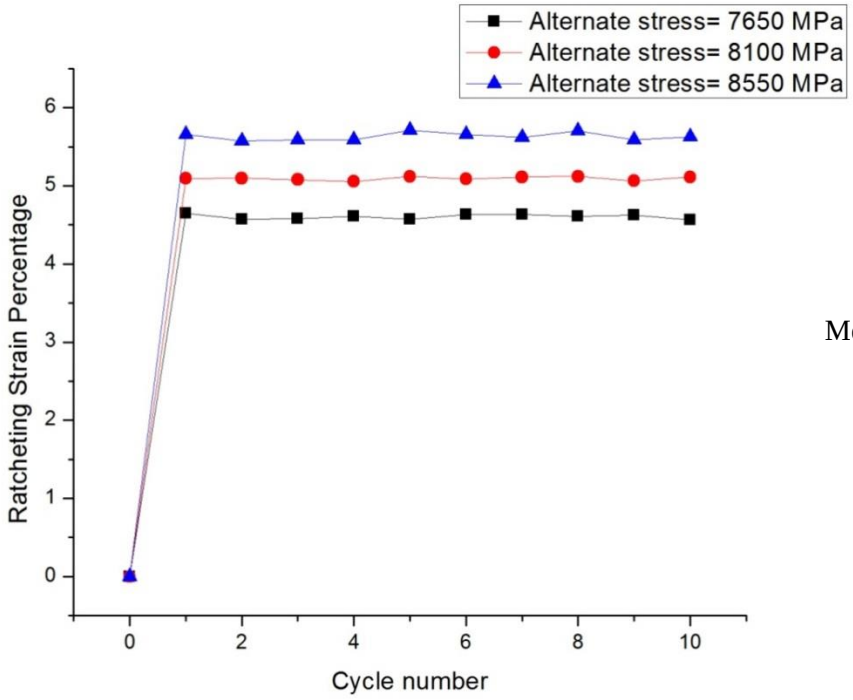

Mean stress = 1080MPa
Fig. 4.5

Copper

The nature of variations of ratcheting strain which is getting accumulated in cyclic loading with increasing number of cycles for varying alternate stress at constant mean stress levels of 1600 and 2400MPa are shown in Fig. 4.6 – Fig. 4.7. In this case also similar nature of strain accumulation was observed. All the investigated cyclic loading tests of Copper are up to five cycles.

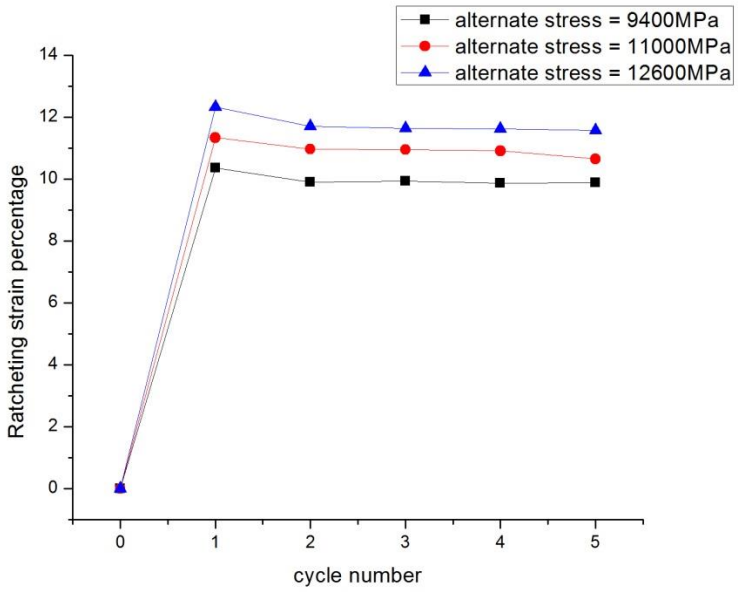

Mean stress = 1600MPa
Fig. 4.6

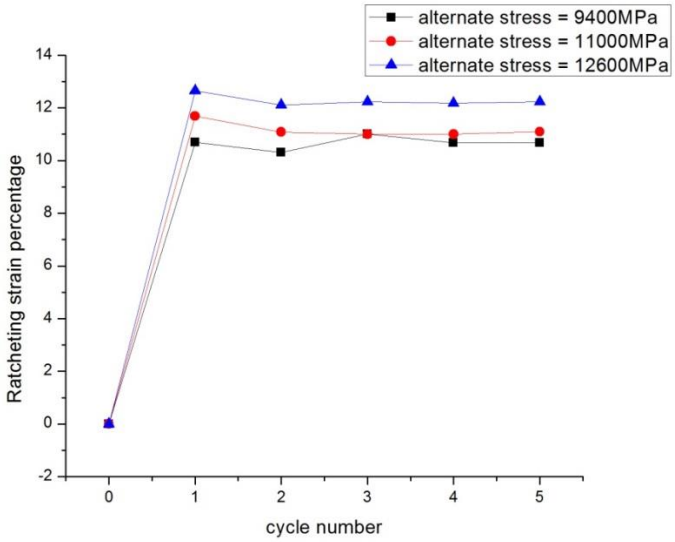

Mean stress = 2400MPa
Fig. 4.7

A closer comparison of strain accumulation for aluminum and copper indicate that copper accumulates more strain as compared to aluminum. The maximum accumulation of ratcheting strain for aluminum is 5.6%, whereas for copper it is 12.2%. A typical plot is given in Fig. 4.8.

It is known that aluminum is having high stacking fault energy (SFE), whereas copper possesses lower SFE. It is described by Dutta and Ray [28] that higher value of SFE generates mobile dislocations into the substructure of the material during deformation, and eventually leads to a stable configuration. This stable configuration of substructure does not allow accommodation of further strain to the material. Therefore aluminum is having lower strain, whereas copper can accommodate some more strain than aluminum before stabilization.

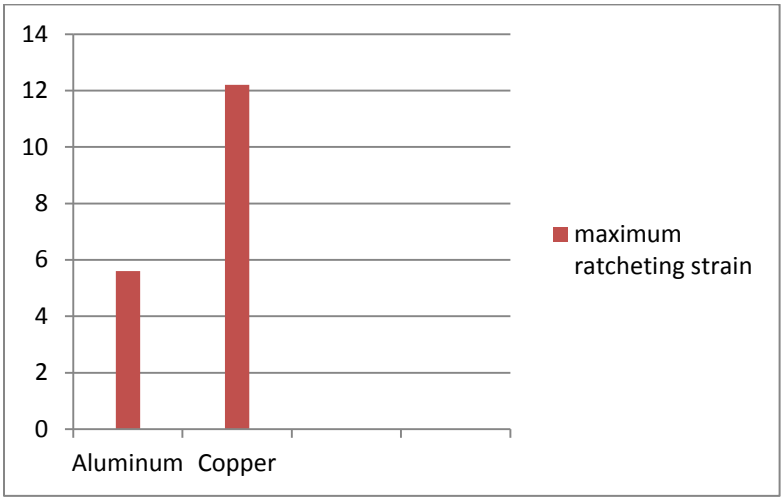

Fig. 4.8

4.3 Strain accumulation under varying stress amplitude at constant mean stress:

Aluminum

The variations of ratcheting strain accumulated in cyclic loading with increasing number of cycles for varying mean stress at constant alternate stress levels of 7650, 8100 and 8550 MPa are shown in Fig. 4.09 – Fig. 4.11. The results in these figures indicate that ratcheting strain $\square_r$ increases quickly in the initial cycle, and then it almost negligibly increases in magnitude. This nature of strain increment was found for all the investigated stress combinations. It can also be stated that at a constant alternate stress and at any specific N value, the magnitude of total

accumulated ratcheting strain increases with increasing stress amplitude. All the investigated cyclic loading tests are up to ten cycles.

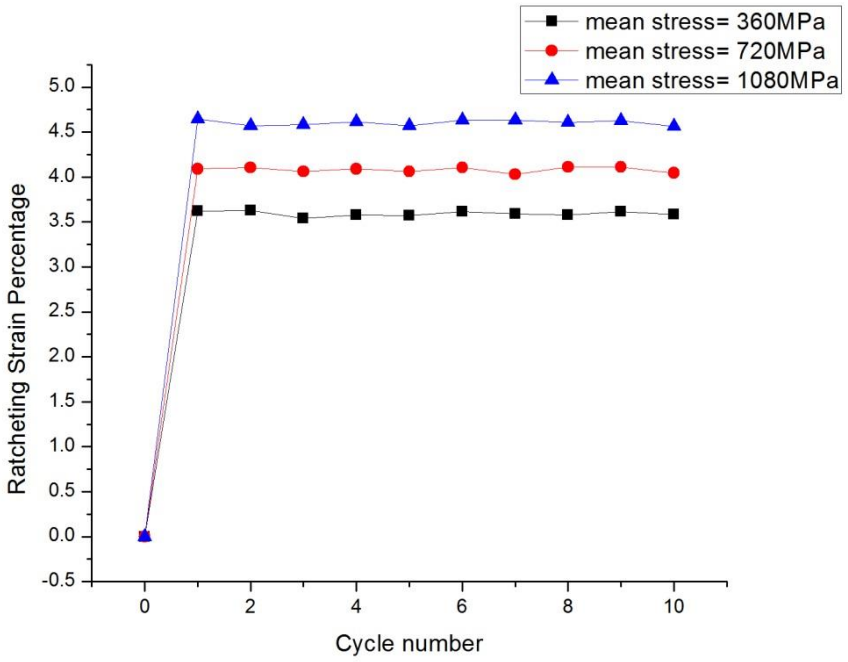

Alternate stress = 7650MPa

Fig. 4.9

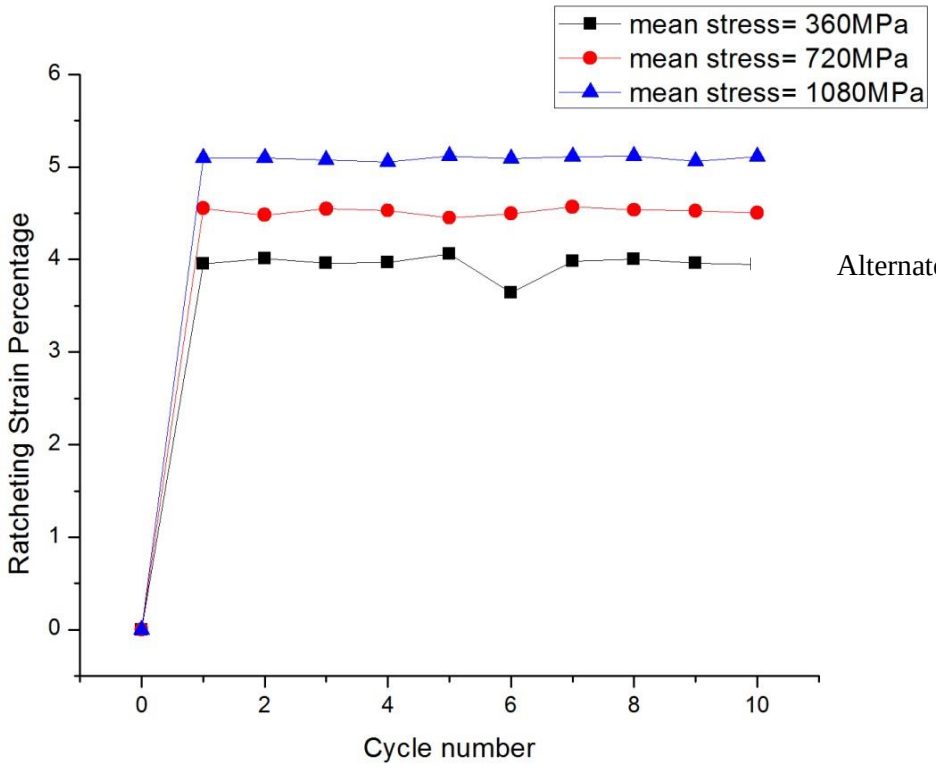

Alternate stress = 8100MPa

Fig. 4.10

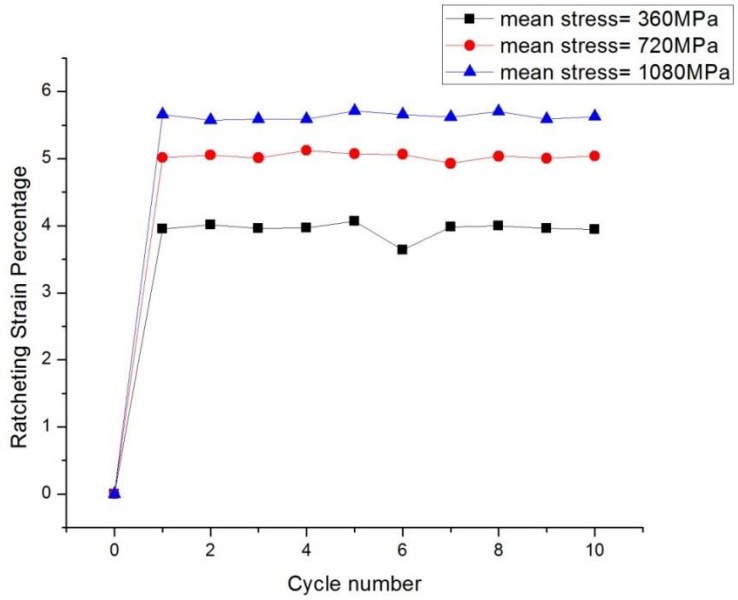

Alternate stress = 8550MPa

Fig. 4.11

Copper

The following curves show the variation of ratcheting strain of copper with varying mean stress and constant alternate stress.

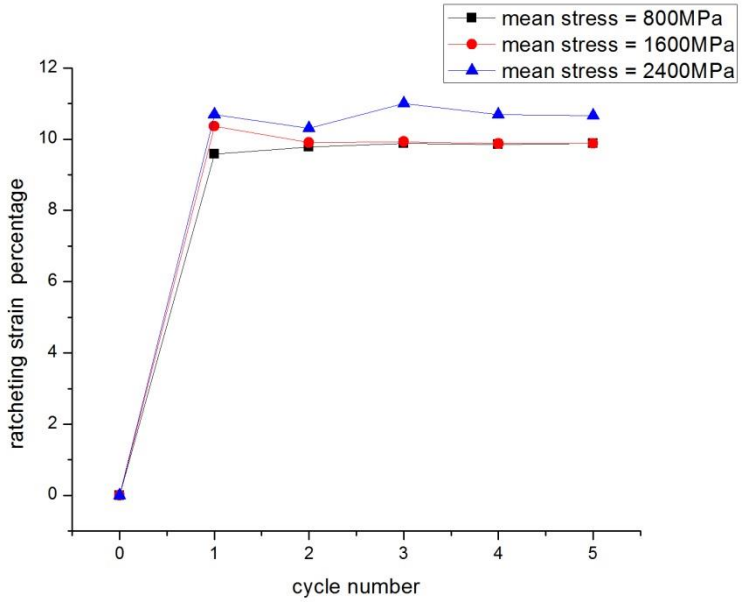

Alternate stress = 9600MPa

Fig. 4.12

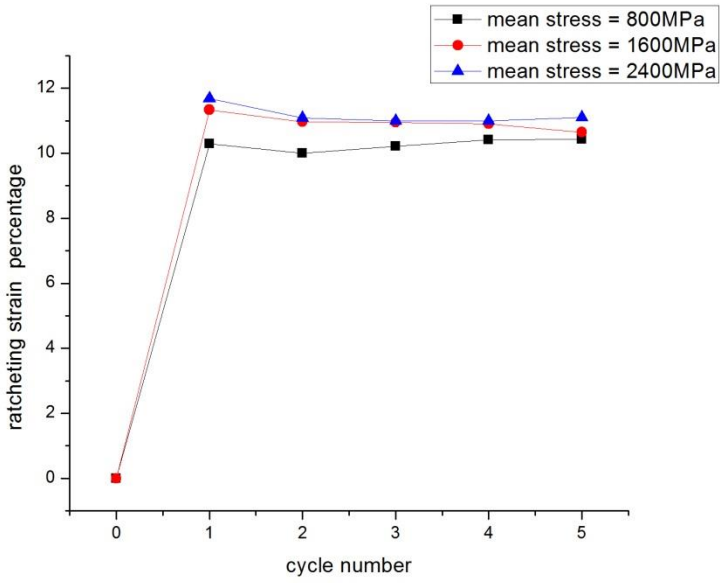

Alternate stress = 11200MPa

Fig. 4.13

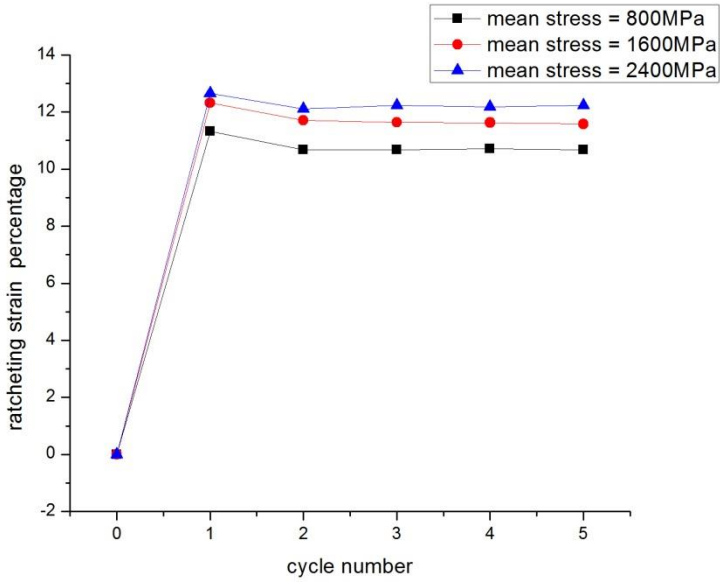

Alternate stress = 12800MPa

Fig. 4.14

4.4 Effect of temperature on strain accumulation:

It is known that strength of materials vary when the working temperature varies from sub-zero to elevated temperature. To reveal the variation of strain accumulation at various temperatures, a few fatigue tests were conducted at temperatures 200K, 300K, 400K and 500K. It was noticed

that simulated specimens break at the very first cycle at a temperature of 500K. For all other cases, specimens accumulate different amount of stain, as is shown in Fig. 4.15- Fig. 4.16.

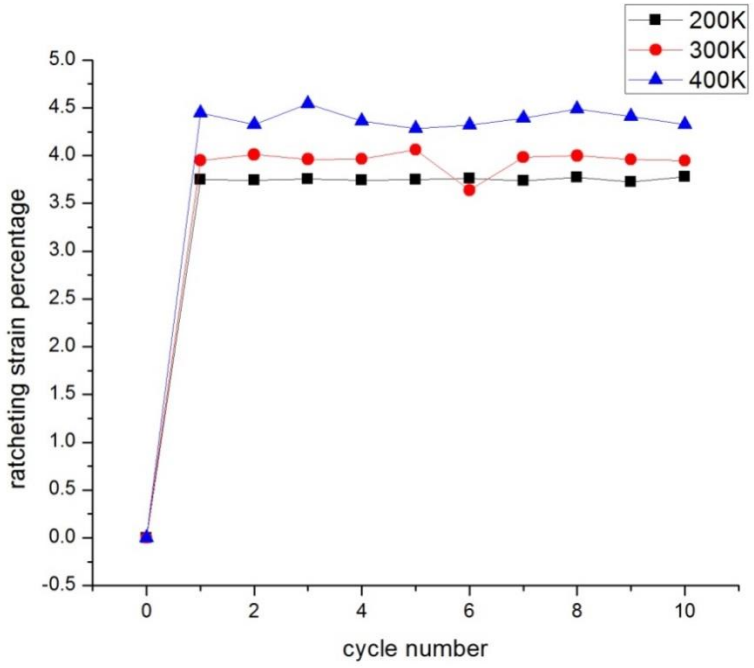

Aluminum

Fig. 4.15

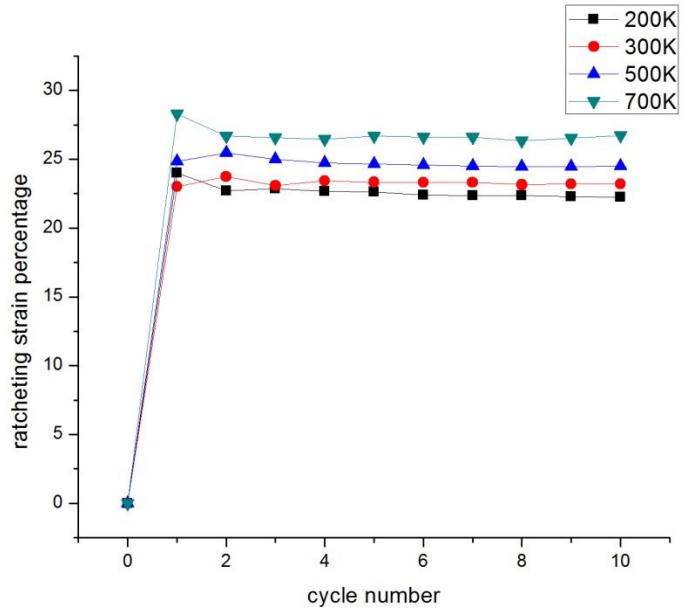

Copper

Fig. 4.16

4.5 Stages of Fatigue failure

Stages of Fatigue failure observed by simulation of the Copper box [20 50 20] at stress range [16500MPa, -10400MPa]. Failure crack occurred at 10^{th} cycle. VMD (Visual Molecular Dynamics) images show the stages to failure.

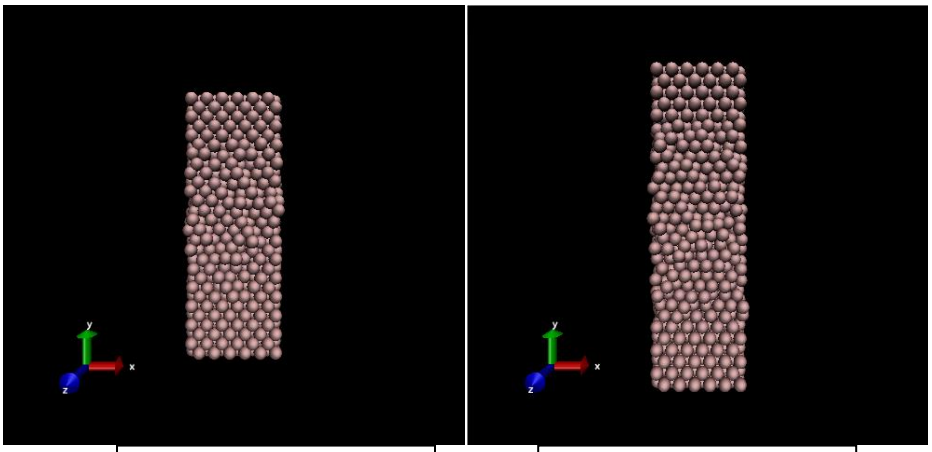

NO LOAD CONDITION

ELONGATION

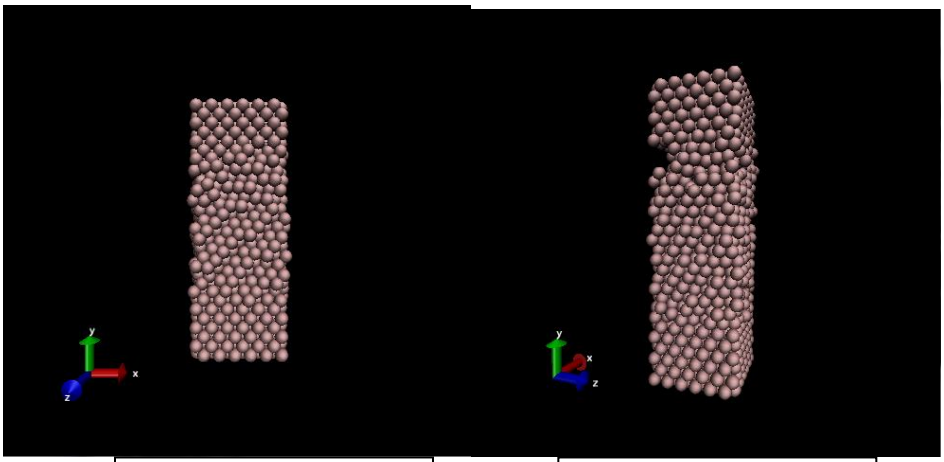

COMPRESSION

CRACK INITIATION

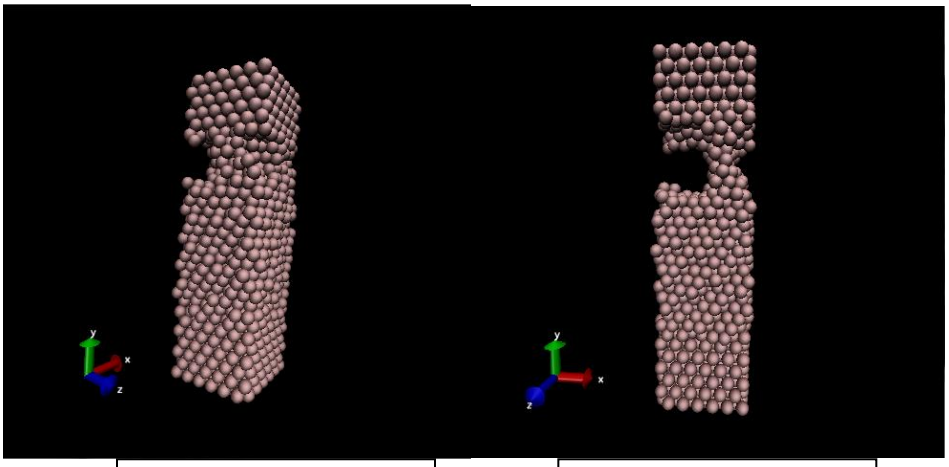

CRACK GROWTH | DUCTILE FRACTURE

Given below are the cyclic loading curve and Stress-Strain hysteresis loop for above mentioned copper box at stress range [16500MPa, -10400MPa]. Mean stress = 2400MPa and Alternative stress =13450 MPa

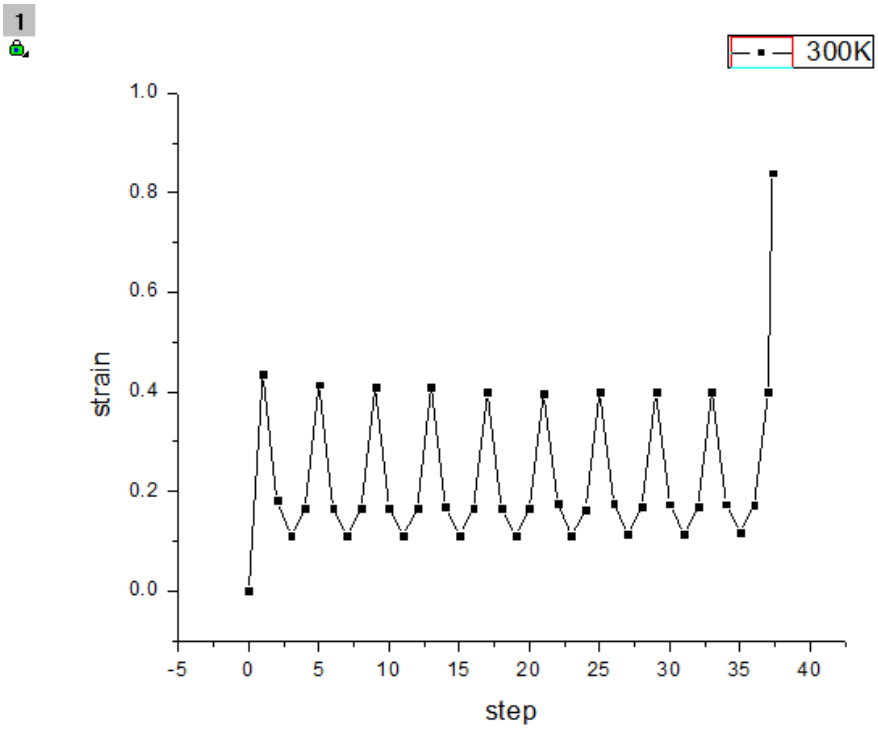

Cyclic loading curve

[16500MPa, -10400MPa]
Mean stress = 2400MPa
Alternate stress = MPa
Fig. 4.17

4.6 Comparison of simulation results with practical results

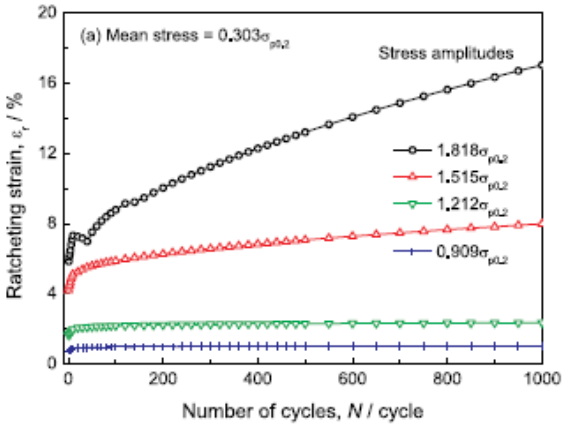

Results obtained from practical experiments[29]

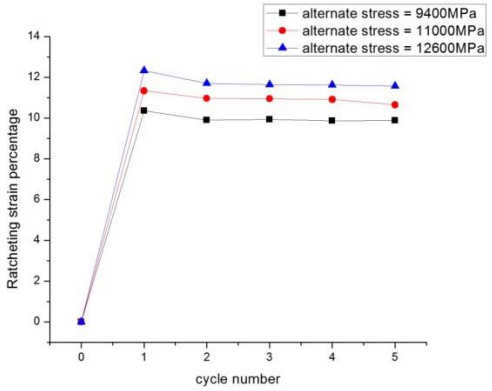

Copper

Results obtained from MD simulation

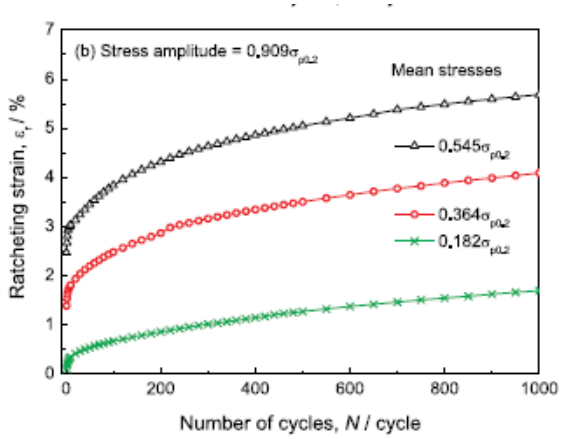

Results obtained from practical experiments

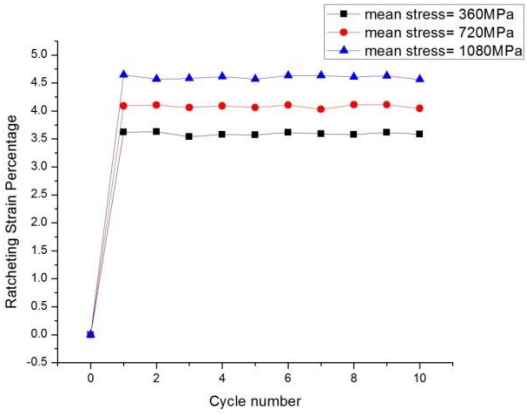

Aluminum

Results obtained from MD simulation

The comparison of results obtained from practical experiments to that from simulations show almost similar ratcheting behavior in both cases. The final ratcheting strain obtained from both routes are close.

Chapter 5

Conclusion

From this research work based on computer simulations, we could conclude that

1. With constant mean stress, ratcheting strain of materials tested increases with increase in the alternate stress value.
2. With constant alternate stress, ratcheting strain accumulated increases with increase in mean stress values.
3. This can be explained by materials stacking fault energy.
4. With increasing temperature of simulation there is rise in ratcheting strain of the materials tested.
5. Molecular dynamics can be a very effective way of simulating ratcheting behavior of materials.it is a very effective tool.

6. References

1. The Alexander L. Kielland accident, Report of a Norwegian public commission appointed by royal decree of March 28, 1980, presented to the Ministry of Justice and Police March, 1981 ISBN B0000ED27N
2. George E. Dieter, Mechanical Metallurgy (page no. 246)
3 M.D. Ruggles, E. Krempl, J. Mech. Phys. Solids 38 (1990) 575–585.
4 F. Yoshida, Int. J. Pres. Vessel Piping 44 (1990) 207–223.
5 T. Hassan, S. Kyrikides, Int. J. Plast. 10 (2) (1994) 149–184.
6 R.J. Rider, S.J. Harvey, H.D. Chandler, Int. J. Fatigue 17 (7) (1995) 507–511.
7 Z. Xia, D. Kujawski, F. Ellyin, Int. J. Fatigue 18 (1996) 335–341.
8 U.C. Ozgen, Mater. Des. 29 (2007) 1575–1581.
9 N. Isobe, M. Sukekawa, Y. Nakayama, S. Date, T. Ohtani, Y. Takahashi, N.Kasahara, H. Shibamoto, H. Nagashima, K. Inoue, Nucl. Eng. Des. 238 (2008) 347–352.
10 S.C. Kulkarni, Y.M. Desai, T. Kant, G.R. Reddy, Y. Parulekar, K.K. Vaze, Int. J. Press. Vessels Piping 80 (2003) 179–185.
11 X. Feaugas, C. Gaudin, Int. J. Plast. 20 (2004) 643–662.
12 C. Gaudin, X. Feaugas, Acta Mater. 52 (2004) 3097–3110.
13 W. Liu, Z. Gao, Z. Yue, Mater. Sci. Eng. A 492 (2008) 102–109.
14 G.Z. Kang, Q. Gao, X.J. Yang, Int. J. Mech. Sci. 44 (8) (2002) 1645–1661.
15 G.Z. Kang, Y.G. Li, J. Zhang, Y.F. Sun, Q. Gao, Theor. Appl. Fract. Mech. 43 (2005) 199–209.
16 P. Delobelle, P. Robinet, L. Bocher, Int. J. Plast. 11 (1995) 295–330.
17 M. Kobayashi, N. Ohno, T. Igari, Int. J. Plast. 14 (1998) 355–372.
18 D. Nouailhas, J.L. Chaboche, S. Savalle, G. Caillet, Int. J. Plast. 1 (1985) 317–330.
19 J.L. Chaboche, Int. J. Plast. 7 (1991) 661–678.
20 C. Holste, W. Kleinert, R. Giirth, K. Mecke, Mater. Sci. Eng. A 187 (1994) 113–123.
21 Y. Jiang, P. Kurath, Int. J. Plast. 12 (1996) 387–415.
22 X. Chen, R. Jiao, Int. J. Plast. 20 (2004) 871–898.
23 S. Bari, T. Hassan, Int. J. Plast. 18 (2002) 873–894.

24 X. Chen, R. Jiao, K.S. Kim, Int. J. Plast. 21 (2005) 161–184.

25 J.L. Chaboche, Int. J. Plast. 7 (7) (1991) 661–678.

26 Paul S.K., Sivaprasad S., Dhar S., Tarafder S., "True stress control asymmetric cyclic plastic behaviour in SA333 C-Mn steel", International Journal of Pressure Vessel and Piping, 87 (2010): pp. 440-446.

27 Chen G., Chen X., Niu C-D, "Uniaxial ratcheting behaviour of 63Sn37Pb solder with loading histories and stress rates", Materials Science and Engineering A, 421 (2010): pp. 238-244.

28 K. Dutta and K K Ray, "Uniaxial Ratcheting Behaviours of Materials with Different Crystal Structures", Published in CD-ROM of the International Conference on Advances in Materials and Materials Processing, ICAMMP, December 9 – 11, 2011 at IIT Kharagpur

29 29 Guozheng Kang et al." Uniaxial Ratcheting Behaviors of Metals with Different Crystal Structures or Values of Fault Energy: Macroscopic Experiments"